Fabrication of battery separator by coating with sulfonated cellulose nanofibrils on kraft paper and inkjet paper substrates

Tillverkning av batteriseparator genom bestrykning med sulfonerad cellulosananofibriller på kraft papper och bläckstråle papper substrat

Forat Alshogran

Faculty of Health, Science and Technology, Chemical Engineering

Master of Science in Chemical Engineering

30 ECTS

Supervisors: Mozghan Hashemzehi (Karlstad university), Sanna Lander (Cellfion)

Examiner: Magnus Lestelius

June 2023

Abstract

Modified nanocellulose have distinctive qualities and have drawn a lot of interest from a variety of fields. It is a natural, sustainable product that is manufactured from plant-based materials like wood and other renewable resources. It is also biodegradable. It is a possible material for battery separators because of its great mechanical strength, flexibility, and ability to create a stable and consistent membrane. Due to the cost of using it as a membrane, it has been investigated in this work to see if it can be coated onto a substrate and used as battery separator. In this work sulfonated cellulose nanofibrils (SCNF) has been used to be coated on kraft paper and inkjet paper using a rod coater. Parameters like concentration, thickness and substrates have been varied in this experiment. Viscosity was measured using Brookfield instrument to measure the viscosity for 0,5% SCNF and 1,5% SCNF. The coating was carried out using a rod coater and varying between two rods to influence the thickness, the coating used concentrations of 0,5% SCNF and 1,5% SCNF and two different substrates, kraft paper and inkjet paper. Thickness was determined to study the effect of the variation in rod. The mechanical strength was tested on the coated paper substrates and compared the results to the noncoated substrates as reference, the mechanical strength showed an improvement with the coated SCNF substrates. Permeance through the Gurley method was studied in order to understand how the coated substrates behaves compared to the noncoated. Contact angle was determined as well to understand the wettability of the coated substrates and how they would behave as separators in zinc ion batteries. The contact angle decreased with increasing concentration of the SCNF which is a result of the sulfonate groups. Cross sections were analyzed using SEM to study the influence of the coating to the substrates. Ionic conductivity was also tested to evaluate the possibility of the coated substrates as separators.

Keywords: modified nanocellulose, coating, battery separator, contact angle, mechanical strength, permeance, ionic conductivity.

Sammanfattning

Modifierad nanocellulosa har utmärkande egenskaper och har rört stort intresse från en mängd olika områden. Det är en naturlig, hållbar produkt som är tillverkad av växtbaserade material som trä och andra förnybara resurser. Det är också biologiskt nedbrytbart. Det är ett möjligt material för batteriseparatorer på grund av dess stora mekaniska styrka, flexibilitet och förmåga att skapa ett stabilt och konsekvent membran. På grund av kostnaden för att använda det som membran har det undersökts i detta arbete för att se om det kan bestrykas på ett substrat och användas som batteriseparator. I detta arbete har sulfonerad cellulosa nanofibriler (SCNF) använts för att bestryka på kraft papper och inkjet papper med en stavbestrykare. Parametrar som koncentration, tjocklek och substrat har varierats i detta experiment. Viskositeten mättes med användning av Brookfield-instrument för att mäta viskositeten för 0,5 % SCNF och 1,5 % SCNF. Bestrykningen utfördes med en stavbestrykare och varierande mellan två stavar för att påverka tjockleken, bestrykningen bestod av koncentrationer av 0,5 % SCNF och 1,5 % SCNF och två olika substrat, kraftpapper och inkjet paper. Tjockleken bestämdes för att studera effekten av variationen i staven. Den mekaniska styrkan testades på de bestrukna papperssubstraten och jämförde resultaten med de obestrukna substraten som referens, den mekaniska styrkan visade en förbättring med det bestrykta SCNF-substraten. Permeans genom Gurley-metoden studerades för att förstå hur de bestyrkta substraten beter sig jämfört med de obestrukna. Kontaktvinkeln bestämdes också för att förstå vätbarheten hos de belagda substraten och hur de skulle bete sig som separatorer. Kontaktvinkeln minskade med ökande koncentration av SCNF som är ett resultat av sulfonatgrupperna. Tvärsnitt analyserades med användning av SEM för att studera inverkan av bestrykningen på substraten. Jonledningsförmåga testades även för att studera möjligheten av de bestryka substraten som separatorer.

Nyckelord: modifierad nanocellulosa, bestrykning, batteri separator, kontaktvinkel, mekanisk styrka, jonledningsförmåga.

Table of contents

1. Introduction

Ion selective membranes are an essential component of numerous large-scale energy storage technologies, including redox flow batteries. The perfluorinated sulfonic substance Nafion dominates these synthetic polymer membranes (Prifti et al 2012). From a sustainability standpoint, it is difficult to produce membranes from petrochemicals and polyfluorinated compounds in particular because of the high price of Nafion (Noack et al 2016). On the approach to green energy storage, finding ways to replace these materials while maintaining the components functionality would be a significant step (Yee et al 2020). In order to cut production costs, enhance functionality, and reduce environmental effect, there has been an increase in interest in trying to replace conventional ion exchange membranes with membranes made of bio-based and renewable materials (Muhmed et al 2020).

In devices like hydrogen fuel cells and redox flow batteries, membranes made from cellulose nanofibrils (CNFs), or nanocrystals have been used as a medium to transport protons. Even at high temperatures, where commercial membranes like Nafion have subpar performance due to dehydration, these materials have a tendency for proton conduction because of the plentiful hydroxyl groups on the fibril- or crystal-surfaces combined with ionic groups introduced via chemical modification (Bayer et al 2016). It has been suggested that oxidatively sulfonated cellulose, which is produced via periodate oxidation and bisulfite sulfonation, is a suitable material for the manufacture of ion-selective membranes for electrochemical energy devices using liquid electrolytes (Lander et al 2022). The resulting cellulose membrane performs two functions. Wet stability is added by the cross-linkable aldehyde groups, while cationic transport is enhanced by the sulfonated groups (Tiina et al 2021). Ion selective membranes are quite expensive and is made out of polymers which is the reason for using porous membranes because they are biodegradable. Ion selective membranes separate certain chemical substances while allowing other chemical substances to pass. Porous membranes on the other hand limits only dendrite growth, meaning that their functionality isn’t as wide as ion selective membranes but functions well as separator. The primary concern however is the membrane production cost which makes the process too expensive because of the long drainage times and therefor is the possibility of coating studied.

Nanocellulose has a high mechanical strength, is flexible, and can form a consistent and stable membrane making it a potential material for battery separators. However, the expensive cost of manufacturing nanocellulose may raise the overall price of the battery's membrane. Nanocellulose is typically created by subjecting cellulose fibers which can come from a variety of sources, including wood, cotton, or plants to mechanical or chemical processing. With numerous phases like pulping, bleaching, and enzymatic treatment, the production process can be complex and energy intensive. The price of labor, equipment, and raw materials can all increase the cost of production. Despite improvements in production technology and scale-up, the price of nanocellulose is still quite high when compared to other polymer materials used in battery separators, such as polyethylene and polypropylene. The high production cost of nanocellulose is one of the difficulties in employing it in coatings. However, it is anticipated that the price will drop making nanocellulose a more affordable material for industrial uses as the technology for creating it continues to advance and scale up (Dieter et al 2018). The compatibility of nanocellulose with other substances such as polymers and adhesives, which are frequently employed in coating applications is another difficulty (Chakrabarty & Teramoto 2018). To increase the performance and stability of the coating researchers are investigating strategies to improve the compatibility of nanocellulose with these substances.

Nanocellulose is a sustainable, natural substance made from renewable resources like wood and other plant components and it is also biodegradable. Due to its superior mechanical and barrier qualities, nanocellulose has been used in coating applications, which is a field of research that is expanding quickly. Nanocellulose is a potential material for coating applications in a variety of industries including packaging, construction, and biomedicine, due to its high strength, stiffness, and transparency (Hubbe et al 2017). When compared to conventional coatings, nanocellulose coatings have a lesser environmental impact and may be more durable and use less material. Nanocellulose is a very adaptable substance that can be created in a variety of ways, including as bacterial cellulose, nanocrystals, and nanofibrils. Each form has distinct qualities and can be applied in different coating situations.

The mechanical strength of nanocellulose coating make them perfect for use in sensitive product packaging, pharmaceutical packaging, and other applications requiring high performance (Aulin et al 2009). Additionally, nanocellulose coatings have great barrier qualities that can help keep moisture and gas from seeping through extending the shelf life of products.

Coatings with nanocellulose are an environmentally beneficial substitute for conventional petroleum-based coatings because they are also biodegradable and compostable. They are suitable for use in packaging applications where lowering the environmental effect is a concern because of this feature (Reeba et al 2022). Furthermore, nanocellulose is a sustainable alternative for the future due to the renewable nature of the raw ingredients needed to generate it. Nanocellulose has a lot of promise to be used as a coating material across many sectors. It offers a promising substitute for conventional coatings and is a material to keep an eye on in the future thanks to its distinctive combination of mechanical, barrier, and environmental qualities. Producing separators for batteries of nanocellulose in an inexpensive way, therefor the processability of coating is examined in this thesis.

1.1 Aim

The aim is examining the potential for producing separators by coating paper substrates with chemically modified nanocellulose. The goal is for the separators to possess characteristics that make them appropriate for usage in various applications, such as zinc/lithium ion batteries, where it has been demonstrated that a combination of strong ionic conductivity and sufficient barrier qualities to inhibit dendrite growth is beneficial (Zhenglin et al 2022).

- Investigate how well the coated substrates can function as separators through ion conductivity measurements, properties that are important in lithium/zinc ion batteries.

2. Cellulose

One of the most prevalent biomaterials on earth is cellulose. Most often plants generate it, but some bacteria can also do it. The homopolymer of glucose found in cellulose is similar to starch, but unlike starch, the glucose monomers are linked together by β -1,4 links.

The sturdy formation of plant cell walls is greatly aided by cellulose, a hard, fibrous, and water-insoluble polysaccharide (Brigham 2018). This arrangement shows that cellulose is a biomaterial with outstanding mechanical qualities and great strength, in addition to assisting in the stability of plant structures.

Cellulose is crucial because it gives the plant cell walls the strength and rigidity, they need to endure the effects of wind, rain, and other environmental pressures. Moreover, cellulose helps to keep the internal balance and health of the plant by facilitating the movement of nutrients and water throughout the plant (Sommerville et al 2005). Since papermaking was first developed in China in the second century BCE, trees have been used as a source of industrial cellulose products. The pulp and paper industry currently consumes a significant amount of cellulose from trees, and other industries are looking into using cellulose for a variety of purposes, such as a renewable alternative to fossil fuels and as a raw material for the creation of advanced materials like nanocellulose.

The way the glucose units are organized gives cellulose its distinctive rigidity and strength. In plants, cellulose synthases are enzymes that are found in the plasma membrane of plant cells and are responsible for producing cellulose (Polko & Kieber 2019). The enzymes extend the cellulose chain by adding glucose units, which is subsequently extruded from the cell and left as a stiff insoluble structure on the cell surface.

Cellulose has a variety of industrial purposes in addition to its natural function in plants, such as serving as a raw material for paper, textiles, and other products, as well as producing biofuels and other renewable resources (Carpita & Gibeaut 1993). D-glucopyranose units are linearly repeated and joined together by the β-(1,4)-glycosidic link to form cellulose which is illustrated in figure 1. Natural cellulose often has alternating crystalline and amorphous parts and is fibrous in morphology. According to a bottom-up method, cellulose synthase (CESA), an enzyme transmembrane complex, produces natural cellulose in plant cells (Lehrhofer et al 2022).

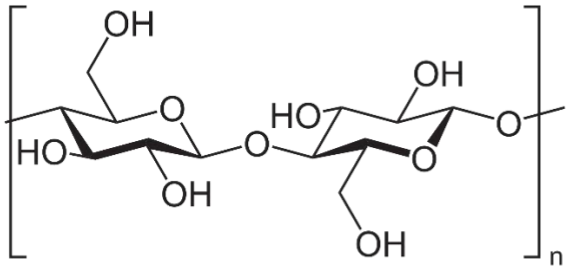

Figure 1: Repetition of cellobiose disaccharide units is used to illustrate the structure of cellulose.

Its renewable forms have been applied as coatings for a variety of things, including packaging, building and transportation supplies, electrical insulation, and water or air filtration. The importance of cellulose in technology is mostly related to the paper industry as well as other cellulose products and derivatives. In response to new material difficulties, industry and academic research has begun to concentrate on the conversion of cellulose into biofuels or other high-value products.

3. Nanocellulose

3.1 Main types of nanocellulose

Since petroleum-based polymers are difficult to degrade, nanocellulose is a significant possibility for replacing petroleum-based polymers in paper and textile coatings. Nanocellulose is the nanometric fibrillar form of cellulose. Various sectors, the scientific community, and politicians are interested in nanocellulose, which comes in the form of rods or fibrils. Its enticing qualities, including high tensile modulus, high specific surface area, and sustainability, account for this current attention. Nanocellulose is additionally frequently regarded as harmless, biocompatible, and biodegradable.

Nanocrystalline cellulose (NCC or CNC), cellulose nanofibrils (CNF), and bacterial nanocellulose (BNC) are the three main kinds of nanocellulose. While all varieties of nanocellulose share a similar chemical composition, variations in sources and extraction techniques result in variations in morphology, particle size, crystallinity, and other properties (Moon et al 2011). Below is a concise overview of each type.

When the fibers are exposed to acid hydrolysis, the amorphous sections of the fibers are destroyed, leaving behind highly crystalline particles with dimensions in the nanoscale range. This process produces nanocrystalline cellulose (CNC) (typically 5-50 nm wide and 100-300 nm long) (Klemm et al 2011). Because of its high mechanical strength, stiffness, and aspect ratio, CNC can be used as reinforcement in a variety of applications, including barrier coatings and polymer composites.

Another form of nanocellulose is called cellulose nanofibrils (CNF), which is created by liberating the small cellulose nanofibrils from the fiber wall and making them to a size that are smaller than those used to create NCC. CNF can be made from a variety of cellulose sources, including cotton, wood pulp, and agricultural waste. Often chemical or mechanical extraction techniques are used to remove the cellulose. After being extracted, the cellulose is processed to get rid of contaminants and cut the cellulose fibers into smaller pieces. In this pre-treatment, techniques including bleaching, beating, or enzymatic hydrolysis may be used (Kargarzadeh et al 2018).

The pre-treated cellulose is next mechanically sheared in order to further degrade the cellulose fibers and disperse them throughout the water. A range of tools, including sonicators, microfluidizers, and high-pressure homogenizers, can be used for this. (Kargarzadeh et al 2018). The cellulose fibers are broken down into smaller pieces by this process, which eventually produces nanofibrils with sizes between 5 and 50 nanometers. Finally, to remove any contaminants or chemicals that may have been added during the pre-treatment or high shear mixing phases, the resulting nanofibrils are routinely washed and cleaned (Dieter et al 2018). After drying, the filtered CNF can be made into a powder or a film.

Bacterial nanocellulose (BNC) produced in a controlled laboratory environment by fermenting particular bacteria including acetobacter xylinum and gluconacetobacter hansenii. (Reshmy et al 2021). BNC is helpful in biomedical and food applications, including as wound dressings, artificial skin, and as a food thickener, thanks to its high purity, high mechanical strength, and strong water-holding capacity (Reshmy et al 2021)

3.2 Modified nanocellulose

Sulfonated CNF will be used as the nanocellulose in this study for fabricating battery separator through coating onto a substrate. Periodate oxidation, the initial step in this procedure, involves treating the pulp fibers with sodium periodate in an acidic solution. The vicinal diols on the surface of the cellulose nanofibrils are selectively oxidized by sodium periodate to produce aldehyde groups. The fibers can then be modified with additional functional groups, such as carboxylic acids or sulfonic acids, by linking them to these aldehyde groups. Sulfonation, the second stage in this procedure involves treating the oxidized fibers with a sulfonating substance, like bisulfite. Sulfonation alters the surface of the CNFs by adding sulfonic acid groups, which can increase their charge density and water solubility (Habibi 2014). In comparison to unaltered fibers, sulfonated cellulose nanofibrils (SCNFs) may also possess improved mechanical, thermal, and biocompatibility characteristics (Liimatainen et al 2012). After oxidation and sulfonation a microfluidizer is used, a high-pressure homogenizer that subjects the substance to strong shear forces, the sulfonated CNFs further processed the fibers to CNFs. The CNFs are subsequently scaled down to the nanoscale, with diameters varying from tens to hundreds of nanometers, as a result of this process.

3.2.1. Application of modified CNF in battery

Sulfonated cellulose nanofibrils (SCNF) a modified variety of nanocellulose have drawn attention because of their distinctive qualities, including increased hydrophilicity and a high surface charge density (Zhanf et al 2018). Sulfo groups are added to the surface of cellulose nanofibrils during the sulfonation process using a variety of techniques, including treatment with sulfuric acid, chlorosulfonic acid, bisulphite and sulfamic acid. By modifying the reaction parameters such as reaction time, temperature, and sulfonating agent concentration, the degree of sulfonation can be regulated.

SCNFs could be used as a separator in lithium-ion batteries, for example. The high surface charge density and improved hydrophilicity of SCNFs have been demonstrated to improve the battery's performance and security. For instance, Zhang et al (2018)'s study showed that

SCNF-based separators outperformed traditional polyethylene separators electrochemically with stronger ionic conductivity and improved cycling stability.

4. Zinc ion batteries (ZIB)

The main active component of a zinc-ion battery's anode is zinc. Zinc ions (Zn^{2+}) flow through the electrolyte from the anode to the cathode during the battery's discharge cycle, producing an electrical current. The zinc ions move back to the anode during a battery charge and are kept there until the following discharge cycle. Vanadium oxide (V_2O_5) or manganese dioxide (MnO_2) are frequently utilized as the cathode in a zinc-ion battery (Al-Amin et al 2022). During the charge and discharge cycles of the battery, they may accommodate zinc ions and permit them to pass into and out of the cathode. The electrolyte is a liquid or gel that makes it easier for ions to travel between the anode and the cathode. The electrolyte in a zinc-ion battery is typically composed of salt that has been dissolved in an organic solvent (Jun et al 2019). Conductive additives are frequently added to the electrode materials to improve their conductivity and aid in distributing the zinc ions uniformly across the electrode surface. Examples of these additives include carbon black and carbon nanotubes. A thin layer of material called a separator keeps the anode and cathode from coming into contact and short-circuiting the battery. It prevents electrons from moving while allowing ions to do so (Al Amin et al 2022). Overall, the main elements of a zinc-ion battery are zinc, the cathode material (such as MnO_2 or V_2O_5), the electrolyte, conductive additives, and the separator.

When a zinc-ion battery is in operation, zinc ions travel through an electrolyte solution between the anode and cathode electrodes. The cathode is often made of a substance that can intercalate or absorb the zinc ions, whereas the anode is formed of zinc. Zinc atoms in the anode lose their electrons during discharge and transform into positively charged zinc ions (Zn^{2+}), which move through the electrolyte solution to the cathode. The zinc ions interact with the cathode material there, intercalating or absorbing the zinc ions and releasing electrons as a result (Guozhao et al 2018). Although the zinc ions travel back to the anode through the electrolyte solution, the electrons continue to flow through an external circuit to perform beneficial work. Discharge is the process involved, and it generates electrical energy.

When charging, the procedure is reversed, and the zinc ions are sent back to the anode by an external electrical source. The battery is then recharged and ready to be used again for additional discharge and recharge cycles.

4.1 Battery separators

The separator acts as a physical barrier between the anode and the cathode to keep them apart and avoid a short circuit. It simultaneously permits ions to move through while obstructing electron transport. To ensure the safe and efficient operation of a zinc-ion battery specific specifications for the separator material must be met. High ionic conductivity is required because the zinc ions need to be allowed to pass through the separator while the flow of electrons is blocked. For the battery to be able to generate a high power output a high level of ionic conductivity is necessary (Xiaolong et al 2022). Chemical stability in the presence of the battery's electrolyte, the separator material must be chemically stable. It shouldn't react with the electrolyte or the components of the electrodes because this could cause a reduction in battery capacity or even battery failure. Mechanical strength, the separator must be able to endure the stresses and strains of battery operation including the expansion and contraction of the electrode materials caused by the movement of ions in and out of the battery (Jizhang et al 2022). Low electrical resistance to reduce the internal resistance of the battery and increase efficiency, the separator should have a low electrical resistance. Low cost to ensure that the battery's overall cost is competitive with that of existing battery technologies, the separator material should be inexpensive and easily accessible (Jizhang et al 2022).

One of the crucial characteristics to be considered when utilizing sulfonated cellulose nanofibrils (SCNF) as a separator in batteries is ionic conductivity. Ionic conductivity describes the separator's capacity to permit ions to move through it, which is necessary for the battery to operate properly. The following equation can be used to calculate the ionic conductivity:

$$\sigma = L/(R \times A) \qquad [1]$$

Where σ is the ionic conductivity expressed in S/cm, L is the thickness of the separator in cm, R is the resistance measured by the conductivity meter in ohms and A is the cross sectional area of the separator in cm^2.

Because it directly impacts the battery's performance, the separator's ionic conductivity is a crucial factor to consider. Ions can flow through the separator more quickly with a higher ionic conductivity, which could lead to faster charge and discharge rates and a higher energy density. In contrast, a lesser ionic conductivity can result in a battery that performs worse and has a shorter cycle life. (Lander et al 2022)

The resistance of the separator is a crucial factor to consider while utilizing SCNF as a separator. Using Ohm's law, the separator's resistance may be calculated.

$$R = \rho \times (L/A) \quad [2]$$

Where R is the resistance in ohms, ρ is the resistivity of the separator material in ohm-cm, L is the thickness of the separator in cm, and A is the cross-sectional area of the separator in cm^2.

The resistance of the separator is important because it affects the overall resistance of the battery. This may have an impact on the battery's effectiveness and performance. A battery can produce more power and have a longer cycle life if its resistance is lower.

5. Coating and different coating methods

Sulfonated cellulose nanofibrils (SCNF) has been actively explored for application in coatings due to its unique features, such as high aspect ratio, high strength, high surface area, and biodegradability. In terms of mechanical characteristics, water resistance, gas barrier properties, and adhesion, SCNF can improve the performance of coatings.

According to a study by Bayer et al. (2021), SCNF can enhance the coated films mechanical characteristics, including tensile strength, Young's modulus, and elongation at break. The study also discovered that the addition of SCNF can enhance coatings water resistance producing films that are more impermeable to water. Syverud et al. (2013) studied the usage of SCNF as a binder in coatings for food packaging applications. The study discovered that SCNF not only provided a gas barrier that might increase the shelf life of packaged foods, but also enhanced the adhesion of coatings to diverse substrates, including paper and plastic. In one study, SCNF was added to a polyurethane coating to increase its tensile strength and elastic modulus, according to Moon et al. (2011).

For coating SCNF on a paper substrate to be utilized as a separator in batteries, a variety of coating techniques can be used. Each technique has advantages as well as disadvantages.
A quick and efficient coating technique called dip-coating involves dipping the paper substrate into a SCNF dispersion. You can make the SCNF dispersion by dilution SCNF in water or other solvents. After that, the coated paper is dried in the open air or in a controlled atmosphere. Dip-coating is appropriate for small-scale production because it enables fine control over the amount of SCNF put on the paper substrate.

Spray coating is a quick and efficient coating process., which entails utilizing a spray cannon to apply SCNF dispersion to the paper substrate. Typically, a high-pressure pump or compressed air are used to atomize the SCNF dispersion and create a thin mist that is then applied to the paper substrate. A high-throughput technique that can be used for massive production is spray coating.

In the continuous coating process known as "roll-to-roll coating," SCNF is applied to a paper substrate as it travels through a rod which is the used method in this study.
In the laboratory the coating material is placed Infront of the wire-wound rod as shown in figure 2. The coating material creates a moist film on the paper's surface when the rod moves that corresponds to the wire diameter's thickness.

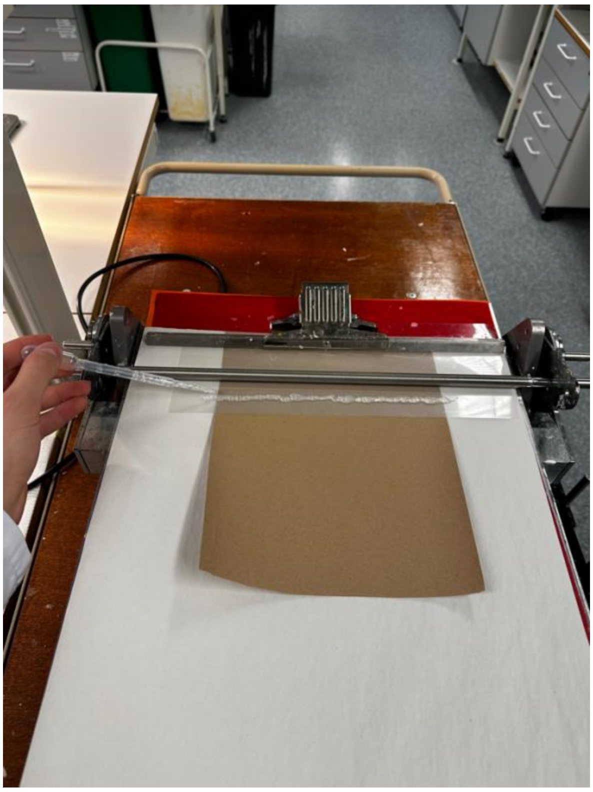

Figure 2: Surface treatment of paper using the rod coating machine.

Although this is not frequently done, the coating substance may also penetrate deeply into the fiber network, changing the paper's surface and bulk properties as seen in Figure 3. This is achieved by using a rod with a fine wire diameter, slow rod movement, a coating mixture with low solid content, and base paper that has a high porosity (e.g. made from unbeaten or slightly beaten fibers). By raising the nip pressure during roll coating, the penetration of the coating suspension is accomplished. The coating mixture's viscosity is another crucial factor that affects how well it penetrates the paper.

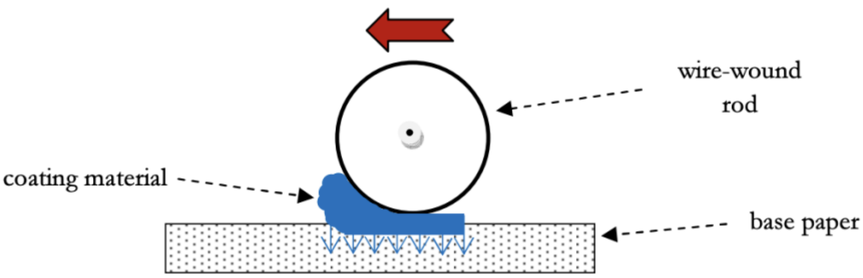

Figure 3: The penetration of the conducting material into the base paper is shown schematically in the rod coating. (Montibon 2011)

6. Experimental part

6.1 Materials

1,5% and 0,5% sulfonated cellulose nanofibrils (SCNF) were supplied by Cellfion which they produced in the laboratory and was given prepared for this study. The concentration is in weight percentage were 1,5g SCNF was added in 100ml to produce 1,5% SCNF and 0,5g in 100ml to produce the 1,5% SCNF.

Further information about how the modified nanocellulose was produced can be found in Sanna Landers research paper (Lander et al 2022). Kraft paper with a grammage of $85g/m^2$and double-sided coated paper (DCP) inkjet paper with a grammage of $250g/m^2$ was provided as substrates by Cellfion.

6.2 Methods

6.2.1 Viscosity measurement

The viscosity of SCNF was measured with the Brookfield viscometer. The SCNF solution was poured into a beaker and placed under the viscometer. The viscometer was set to work with spindle 6 at a speed of 100RPM and was lowered down into the beaker so that the viscosity can be measured. The viscosity was noted every minute for 6 minutes.

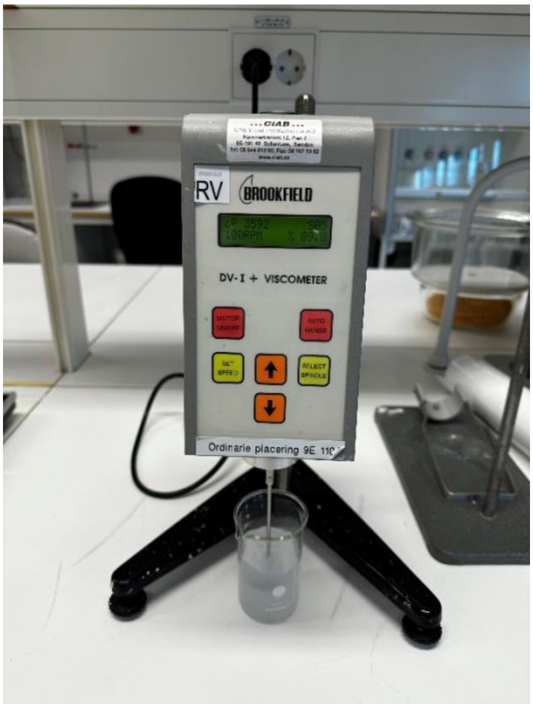

Figure 4: The Brookfield viscometer used for the viscosity measurement.

6.2.2 Coating

A rod coater, K202 Control Coater RK Print Coat Instruments Ltd., Royston, UK was used to coat the paper substrate which is shown in figure 2. The substrate was placed and then a thin film was attached over, and a clamp secured them in place. A pipette was used to spread the sulfonated cellulose nanofibrils over the thin film in front of the wire-round rod. A rod was chosen depending on the thickness of the coating and the velocity was set to 4. After starting the coating machine, the rod would roll over and coat the substrate with the modified nanocellulose. Two different rods were chosen for this experiment, an orange rod and a blue rod where the blue rod had wider wire diameter. The wet film deposit for the orange rod is 60micron and 100micron for the wider blue rod. After the coating the coated substrate was dried using an oven for 2 minutes at 80°C, the dried substrate was stored at 23°C and 50% RH.

6.2.3 Thickness measurement on the substrate

For the different coated substrates, the STFI-thickness instrument TJT-Teknik AB, Järfälla, Sweden was used to measure the thickness and is illustrated in the figure below. The thickness was measured by allowing the substrate to move through the instrument passing a sensor that could measure the average thickness and the result was displayed on the computer software TJ-Test.

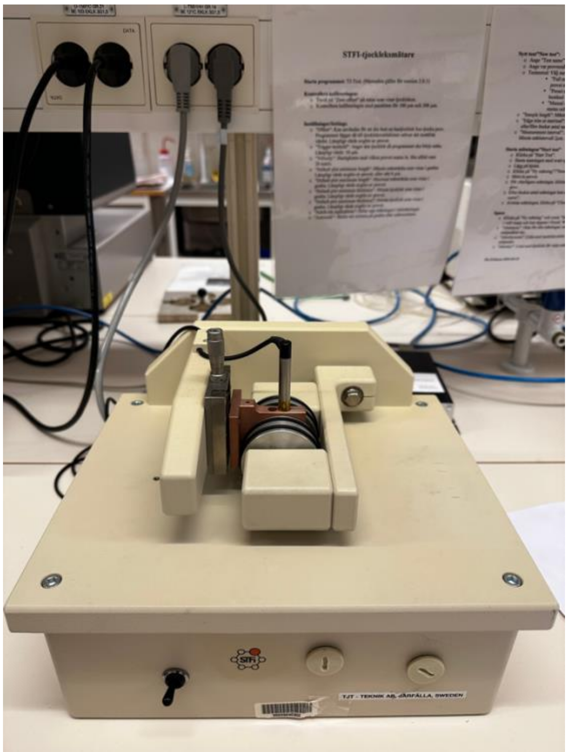

Figure 5: The STFI-thickness measurement used for the coated substrates.

6.2.4 Permeance measurement with Gurley method

The coated substrates were placed under the TMI 58-06 Parker Print-Surf Holland (PPS) machine which measured permeance with the Gurley method. Using an air resistance tester, the Gurley porosity technique evaluates the air permeance of paper. The machine calculates how porous a material is depending on how long it takes for a specific volume of air to travel through the sample. A total of 6 measurements were made on each of the different substrates with different concentrations.

Figure 6: The PPS instrument used to measure permeance through the Gurley method.

6.2.5 Tensile strength

The instrument used was Zwick Roell Z005 tensile testing machine made in Germany and for this experiment the tests was prepared using ISO 1924–3:2011. The sample was cut into multiple stripes before measurement. The sample is then fixed to the apparatus using customized grips created to keep the sample firmly in place throughout testing. A predetermined force is applied to the sample by the machine at a predetermined speed, and the sample's consequent deformation until break is then measured. Tensile stiffness index, tensile index, strain at break and tensile energy absorption results were measured in the testXpert III testing software.

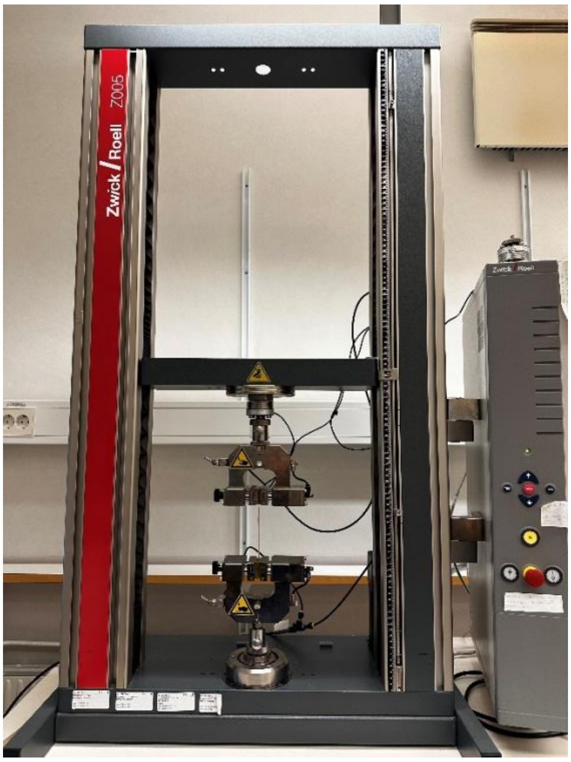

Figure 7: A representation of the Zwick Roell tensile test machine that was used.

6.2.6 Contact angle

The attension theta optical tensiometer Biolin Scientific is a device that can be used to calculate the liquid's contact angle with a solid surface. In many applications, including coating, printing, and adhesion, the wettability of a surface can be determined by the contact angle, which is a crucial characteristic. An image of a water droplet on the surface of interest is taken using a high-resolution camera and the software OneAttension. The shape of the droplet is then examined using image processing methods to calculate the contact angle.

The sample was prepared by mounting the sample on the stage of the attension theta optical tensiometer using double sided tape. With a syringe or other dispensing tool, the liquid droplet is distributed onto the surface. the droplet's volume can be regulated to make sure it is big enough to be seen but not so big that it runs off the surface. An image of the droplet on the surface is taken using the attension theta optical tensiometer 's high-resolution camera. The contact angle is then calculated by the software by analyzing the image. Algorithms are used by the software in the instrument to determine the droplet's shape and calculate the contact angle. Usually, the contact angle is expressed as the average of multiple measurements made at various locations around the droplet's edge. For additional analysis, the contact angle measurement can be stored in a data file or exported to a spreadsheet.

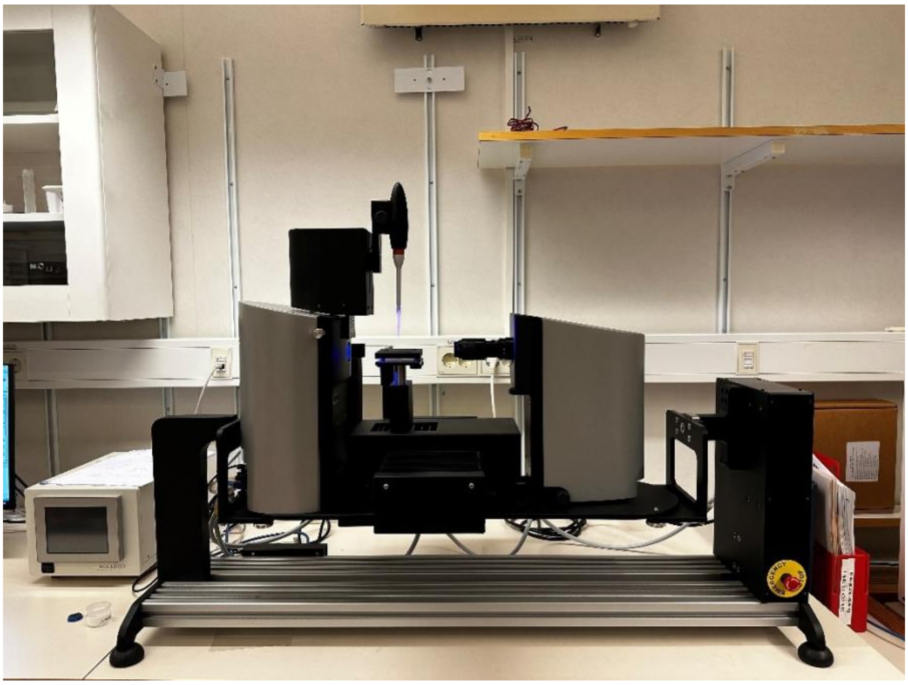

Figure 8: Illustrates the attension theta optical tensiometer that was used to measure contact angle.

6.2.7 Scanning electron microscopy (SEM)

An S-4800 field emission scanning electron microscope (SEM) (Hitachi, Tokyo, Japan) is used for the SEM measurements. The specimen was coated with gold and the voltage used was 1.0kV. The SEM measurements were performed by Cellfion.

6.2.8 Ionic conductivity separator

A Devanathan-Stachurski cell with four electrodes was used because it can measure small resistances in a wide area with water based electrolytes which can be difficult to achieve. The resistance was measured with EIS Gamry potentiostat (electrochemical impedance spectroscopy). The difference method was used where you measure the resistance of the cell without a membrane and subtract that value from the resistance with membrane/separator. The electrolyte was 0,1M KCl and these measurements were done by Cellfion.

Calculations of the ionic conductivity was done and is shown below.

The resistance of the cell without a membrane was $R_{cell} = 51{,}82\ Ohm$ for an open cell, the area was $A = 0{,}5025cm^2$. Calculation for the ionic conductivity of inkjet paper 1,5% SCNF blue coated will be calculated. Three tests were done on the same substrate, but calculations will be shown for one of them as an example.

Using equation [1] to determine the ionic conductivity.

The wet thickness was measured to $L = 404\mu m$ using a Mitutoyo digital micrometer IP65 Japan for the coated area of the substrate, $R_{membrane}$ will be calculated by measuring the resistance in the cell and then subtracting the resistance value without a membrane, therefor $R_{membrane} = R_{tot} - R_{cell} \rightarrow 156{,}5Ohm - 51{,}82Ohm = 104{,}68Ohm$.

The ionic conductivity can now be calculated, $\sigma = \frac{404\times10^{-4}cm}{(104{,}680Ohm\ \times0{,}5025cm^2)\times1000} = 0{,}768mS/cm$

7. Results

The results show two different concentrations 1,5%- and 0,5% SCNF which has been coated on two different substrates, kraft paper and inkjet paper. For the coating machine two different rods where used, a blue rod and an orange rod which indicates the difference in thickness were the blue rod generates a thicker coating layer than the orange rod.

The SEM and ionic conductivity measurements were carried out by Cellfion in Stockholm.

7.1 Viscosity of the SCNF

The mean viscosity of the SCNF solution with the higher concentration was measured to be 3102cp, showing a greater resistance to flow. The greater concentration of SCNF in the solution, which led to additional contacts and entanglements between the nanofibrils, is the reason for this higher viscosity. The mean value of the viscosity of the SCNF solution at reduced concentration, in comparison, was measured to be 13.7cp. This solution's lower viscosity means that it will flow with greater ease.

Table 1: Shows the different viscosity after each minute for the 1,5% concentration SCNF.

Time (min)	Viscosity (cP)
1	3140
2	3100
3	3150
4	3030
5	3030
6	3160
Mean value	3102
Standard deviation	59,13

Table 2: Shows the different viscosity after each minute for the 0,5% concentration SCNF.

Time (min)	Viscosity (cP)
1	16
2	16
3	13
4	12
5	12
6	13
Mean value	13,7
Standard deviation	1,86

7.2 Thickness measurement on the substrates

The noncoated substrates thicknesses were measured to compare with the coated substrates. The results indicated that there was in fact an increase in thickness after coating the substrates with SCNF. The thickness increased with a wider rod.

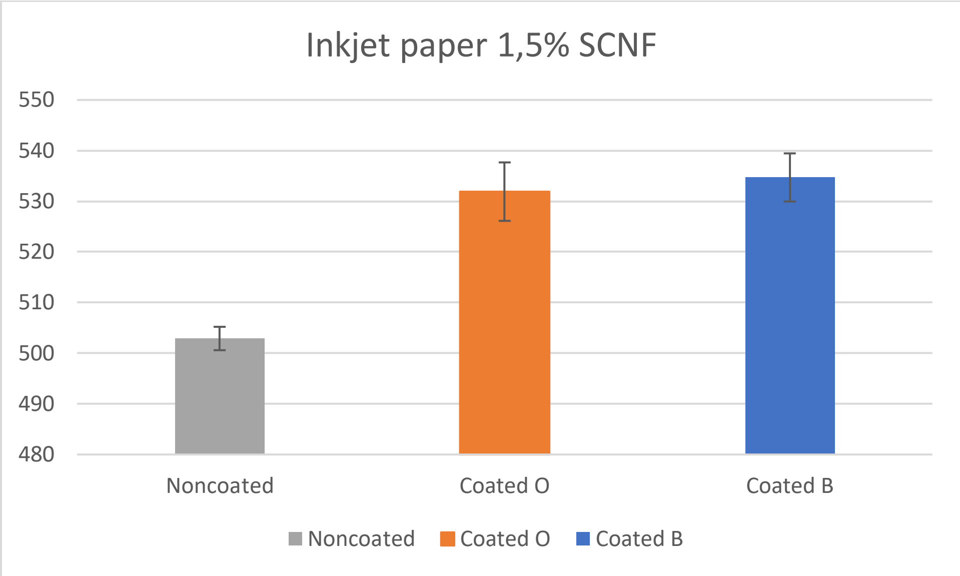

Figure 9: Illustrates the thickness for the ink paper noncoated and with the two different coating rods at 1,5% SCNF concentration.

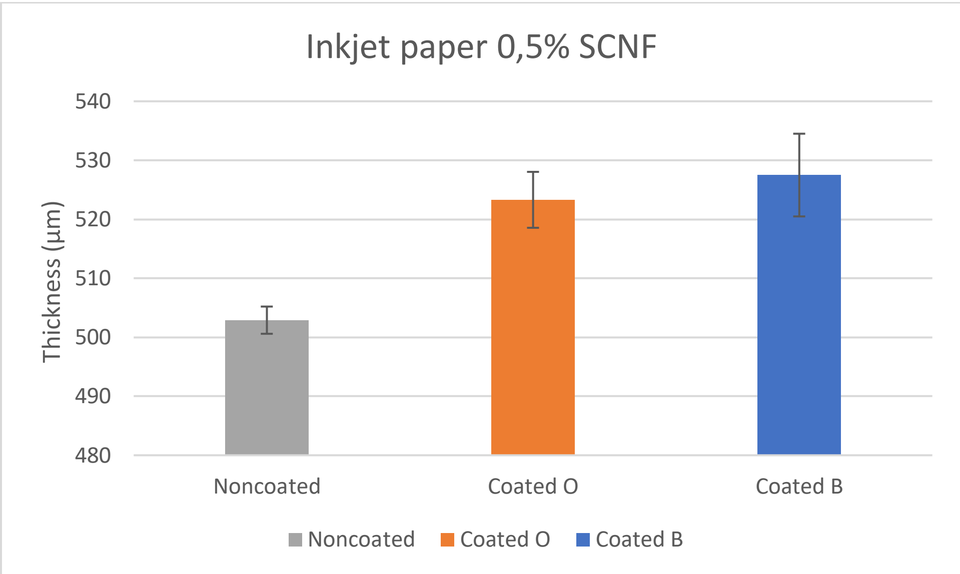

Figure 10: Illustrates the thickness for the ink paper noncoated and with the two different coating rods at 0,5% SCNF concentration.

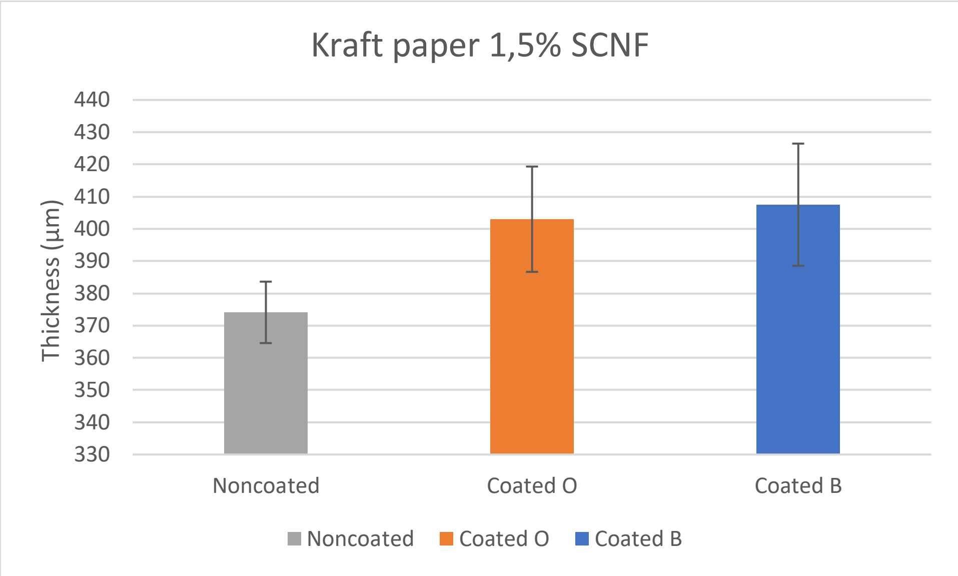

Figure 11: Illustrates the thickness for the kraft paper noncoated and with the two different coating rods at 1,5% SCNF concentration.

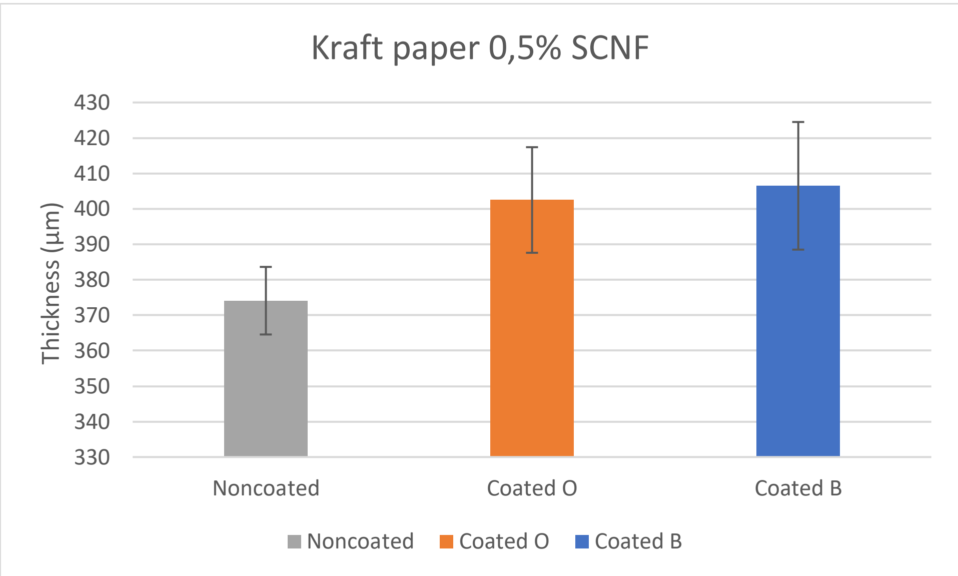

Figure 12: Illustrates the thickness for the kraft paper noncoated and with the two different coating rods at 0,5% SCNF concentration.

7.3 Permeance Gurley

According to the permeance data the coated surface displayed a noticeably higher barrier to air passage than the noncoated paper substrates. A higher value indicates less airflow resistance and thus greater air permeability. The permeance value is expressed in Gurley seconds. This was seen for the inkjet paper's noncoated substrate which showed a higher permeance value, indicating more air permeability. In comparison to the noncoated substrates the coated surface demonstrated improved air passage resistance resulting in decreased air permeability. The existence of the coating layer which functions as a barrier and restricts the passage of air through the substrate is responsible for the increased air barrier property. Since the noncoated kraft paper had a very low air permeability, the device had a hard time providing an accurate measurement within its limitations.

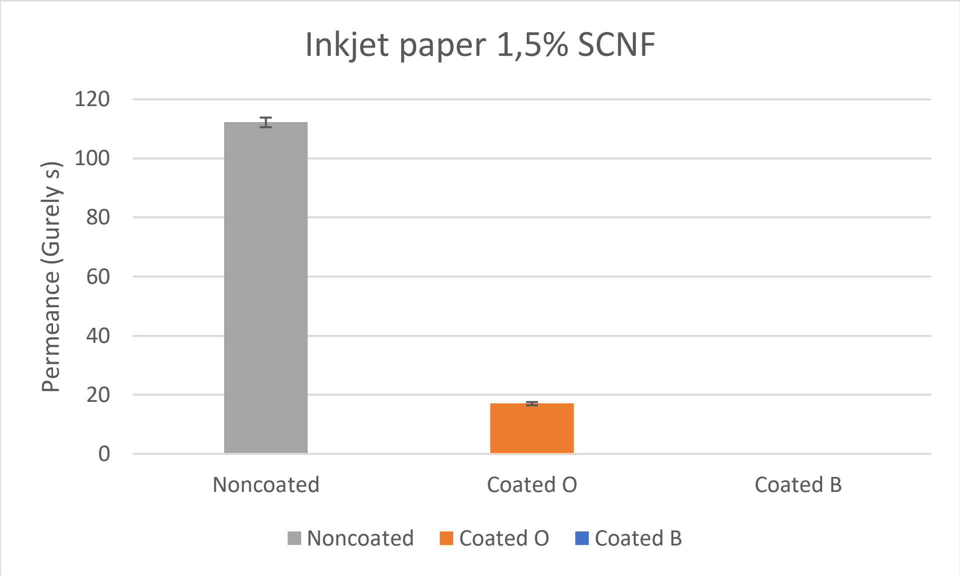

Figure 13: Shows the permeance values for the ink paper noncoated and the two different coating rods at 1,5% SCNF measured with Gurley method.

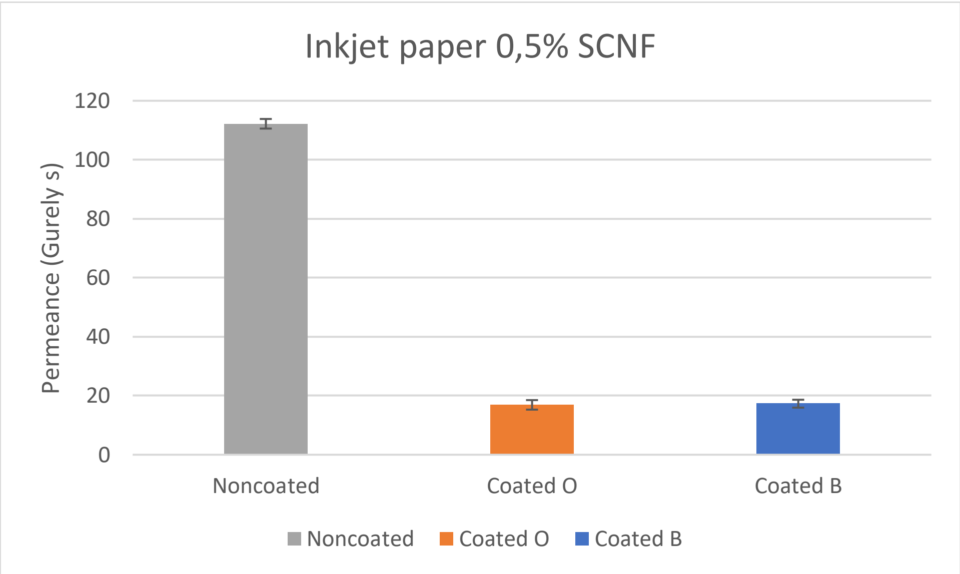

Figure 14: Shows the permeance values for the ink paper noncoated and the two different coating rods at 0,5% SCNF measured with the Gurley method

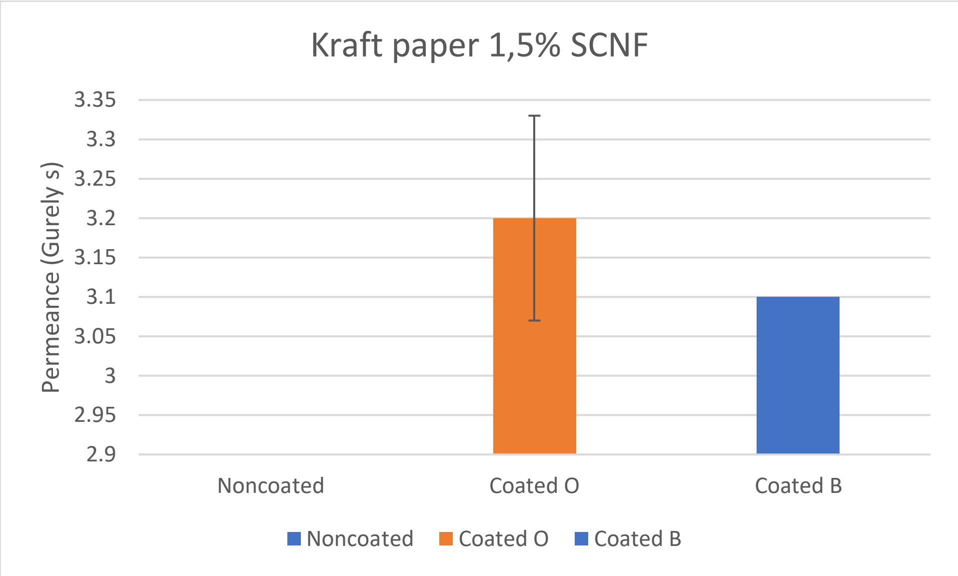

Figure 15: Shows the permeance GURL values for the kraft paper noncoated and the two different coating rods at 1,5% SCNF measured with the Gurley method.

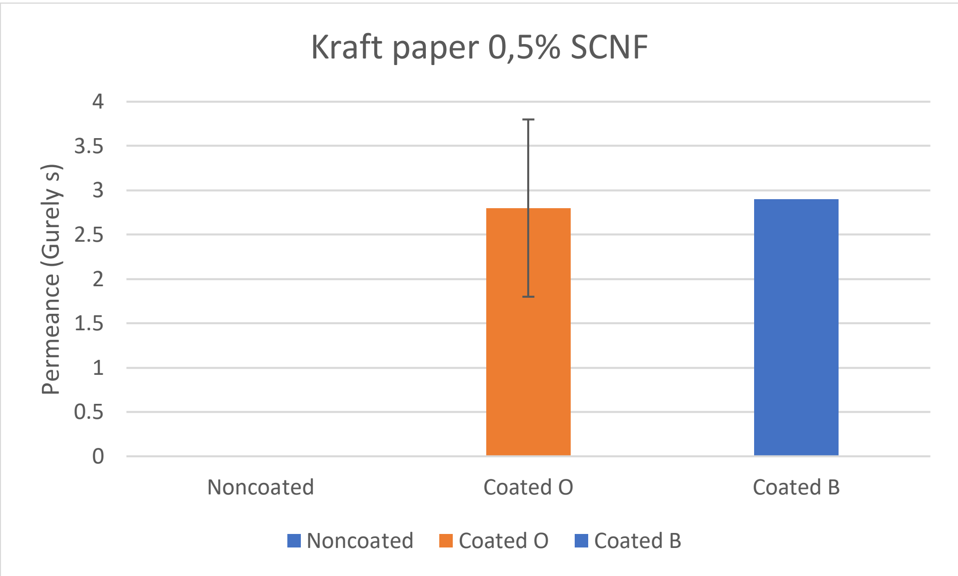

Figure 16: Shows the permeance GURL values for the kraft paper noncoated and the two different coating rods at 0,5% SCNF measured with the Gurley method.

7.4 Mechanical strength

When coated with a 1.5% SCNF solution, the mechanical strength characteristics of both kraft paper and inkjet paper substrates improved. It was interestingly found that a thicker coating produced more mechanical strength. The thicker coating did not however demonstrate greater mechanical strength as compared to the thinner coating in the case of a lower concentration of 0.5% SCNF.

Comparing coated substrates to noncoated substrates, the tensile strength index, energy absorption, and strain at break were all higher for coated substrates. This shows that the SCNF coating improved the substrates overall mechanical performance. The higher energy absorption and strain at break reflect improved capacity to absorb energy and sustain deformation prior to fracture, while the increased tensile strength index shows superior resistance to tensile forces. In contrast, the coated substrates tensile stiffness index decreased. This suggests that after SCNF coating, the substrates rigidity and stiffness will be reduced.

7.4.1 Kraft paper substrate

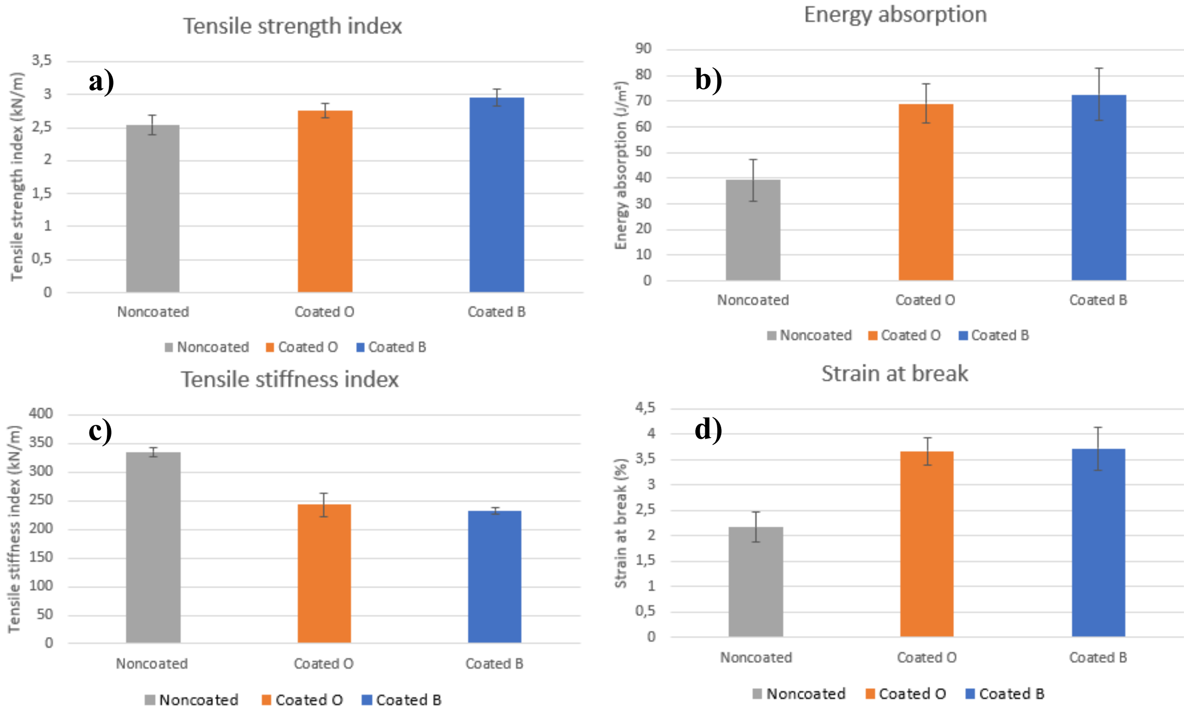

Figure 17: Shows the different mechanical properties for the kraft paper coated with a 1,5% SCNF concentration. (a) describes the tensile strength index, (b) describes the energy absorption, (c) describes tensile stiffness index and finally (d) describes the strain at break.

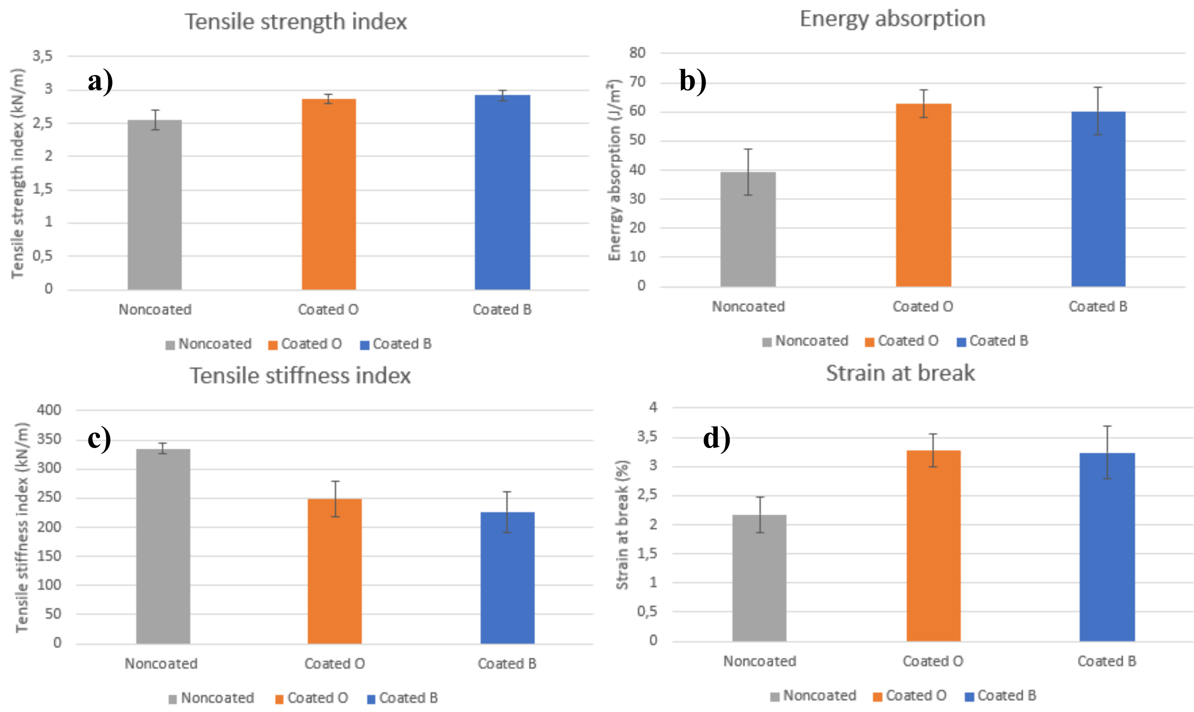

Figure 18: Shows the different mechanical properties for the kraft paper coated with a 0,5% SCNF concentration. (a) describes the tensile strength index, (b) describes the energy absorption, (c) describes tensile stiffness index and finally (d) describes the strain at break.

7.4.2 Inkjet paper substrate

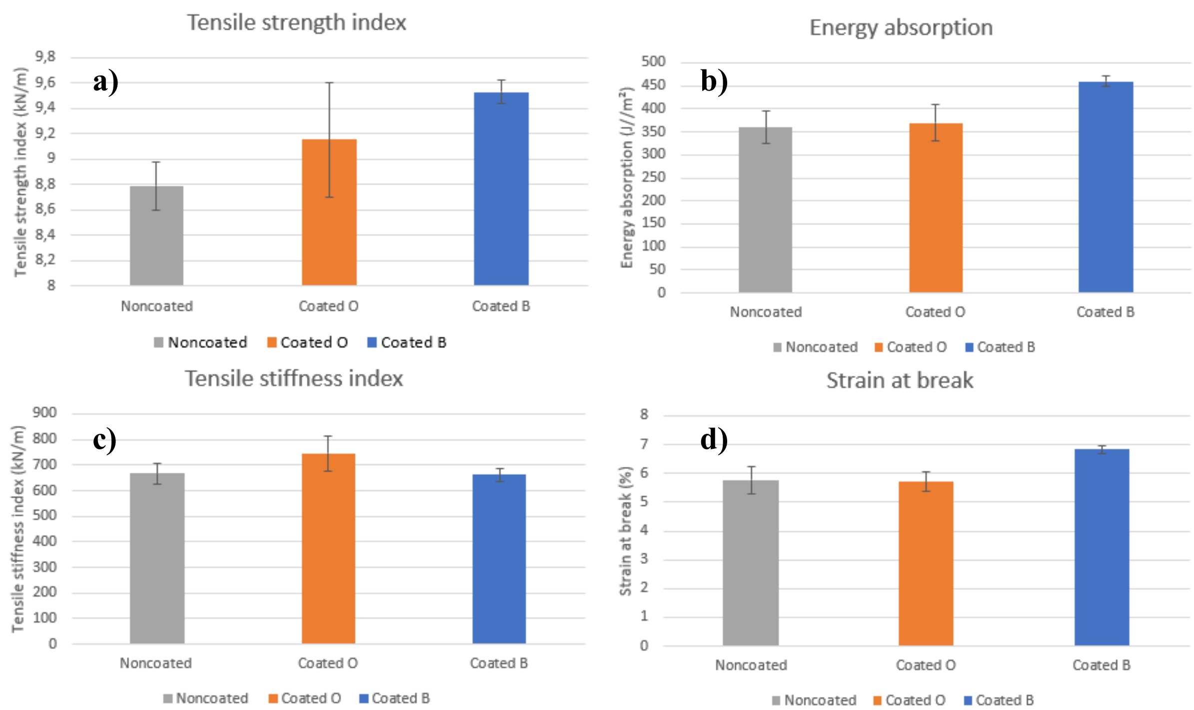

Figure 19: Shows the different mechanical properties for the inkjet paper coated with a 1,5% SCNF concentration. (a) describes the tensile strength index, (b) describes the energy absorption, (c) describes tensile stiffness index and finally (d) describes the strain at break.

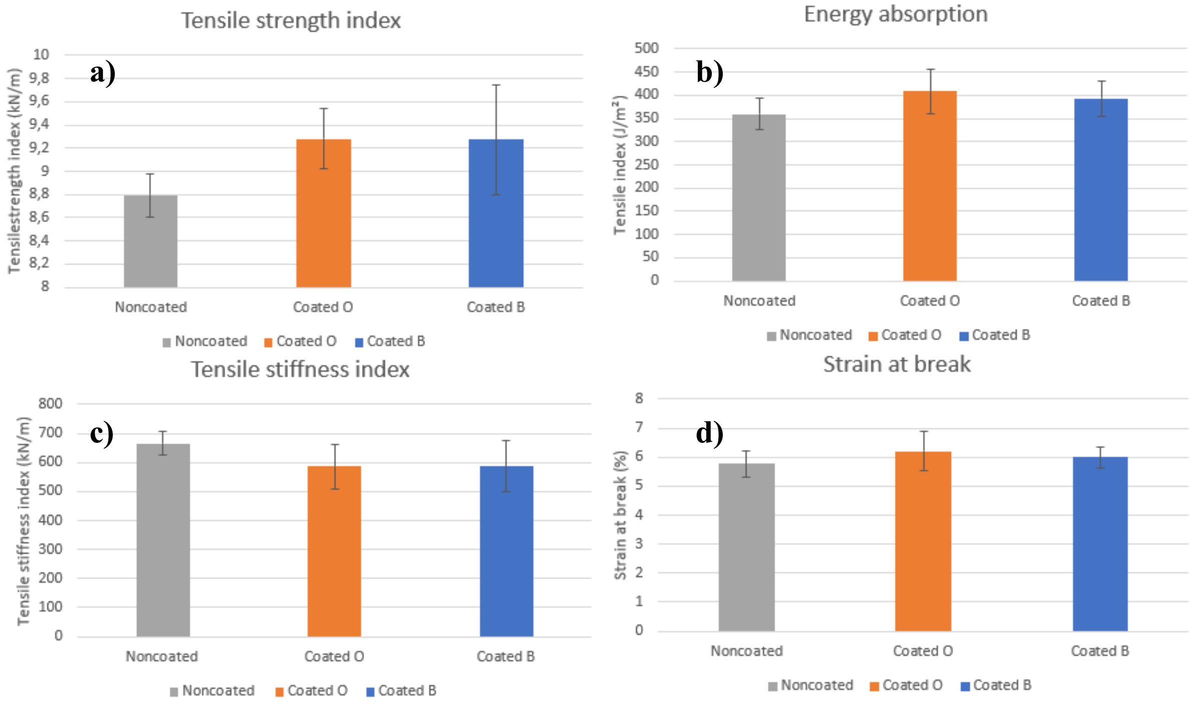

Figure 20: Shows the different mechanical properties for the inkjet paper coated with a 0,5% SCNF concentration. (a) describes the tensile strength index, (b) describes the energy absorption, (c) describes tensile stiffness index and finally (d) describes the strain at break.

7.5 Contact angle for the coated substrates

7.5.1 Kraft paper substrate

Noncoated kraft paper's initial contact angle was found to be 67°. The contact angle decreased noticeably after the 1.5% SCNF coating was applied, reaching values of 25° and 22° for the thinner and thicker SCNF coatings, respectively.

It is notable that the contact angle was also affected by SCNF concentration. Lower SCNF concentrations were found to produce larger contact angles on the coated kraft paper substrates compared to the higher concentration. The thinner SCNF coating's measured contact angles at the lower concentration were 50°, whereas the thicker coating's contact angles were 48°.

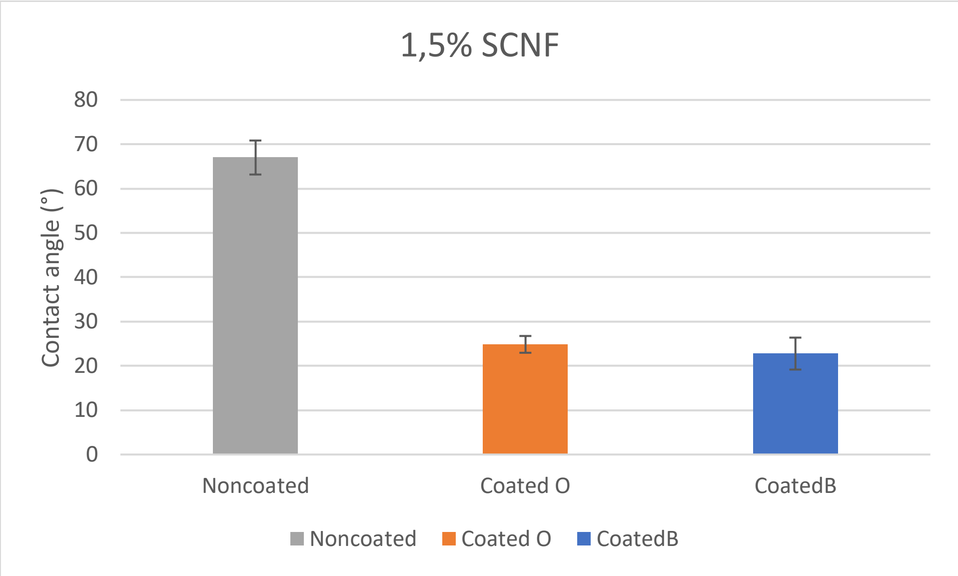

Figure 21: Illustrates the different contact angle values for the noncoated substrate and the two different coating thickness at 1,5% SCNF concentration.

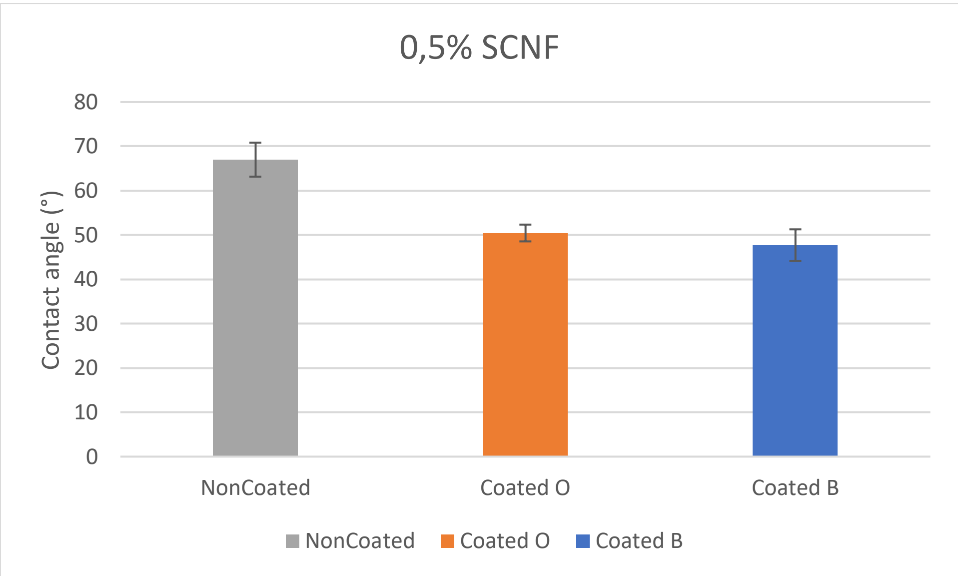

Figure 22: Illustrates the different contact angle values for the noncoated substrate and the two different coating thickness at 0,5% SCNF concentration.

7.5.2 Inkjet paper substrate

It was discovered that noncoated inkjet paper has a 56° initial contact angle. When the SCNF coating was applied, the contact angle reduced similarly to what was seen with kraft paper, with values of 24° and 23° for the thinner and thicker SCNF coatings, respectively. A lower SCNF concentration led to a larger contact angle even for inkjet paper. Specifically, 48° of contact angles were obtained for the thinner SCNF coating at the lower concentration, while

41° of contact angles were measured for the thicker coating. These results show that the SCNF coating on inkjet paper significantly affected the wetting behavior, with higher SCNF concentrations leading to reduced contact angles, indicating increased surface hydrophilicity.

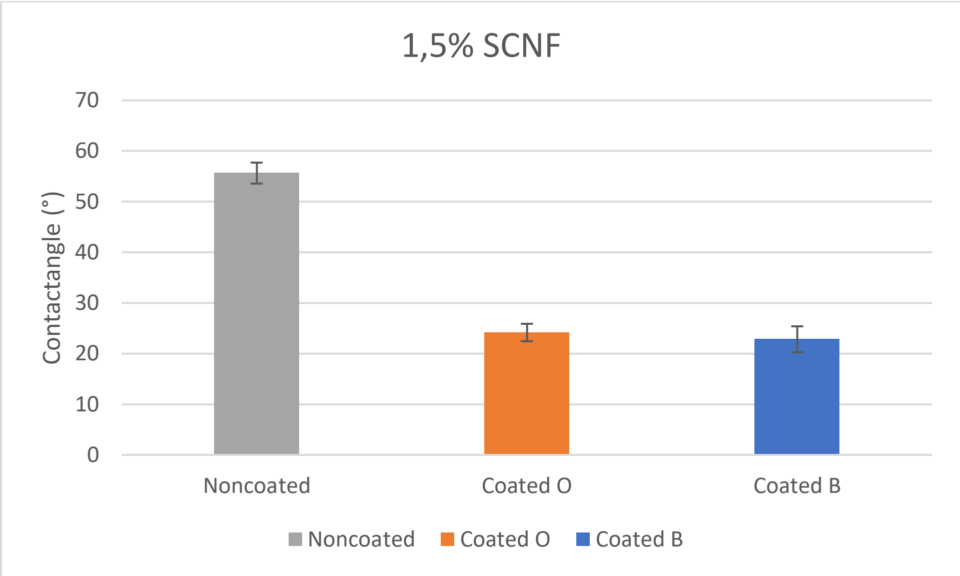

Figure 23: Illustrates the different contact angle values for the noncoated substrate and the two different coating thickness at 1,5% SCNF concentration.

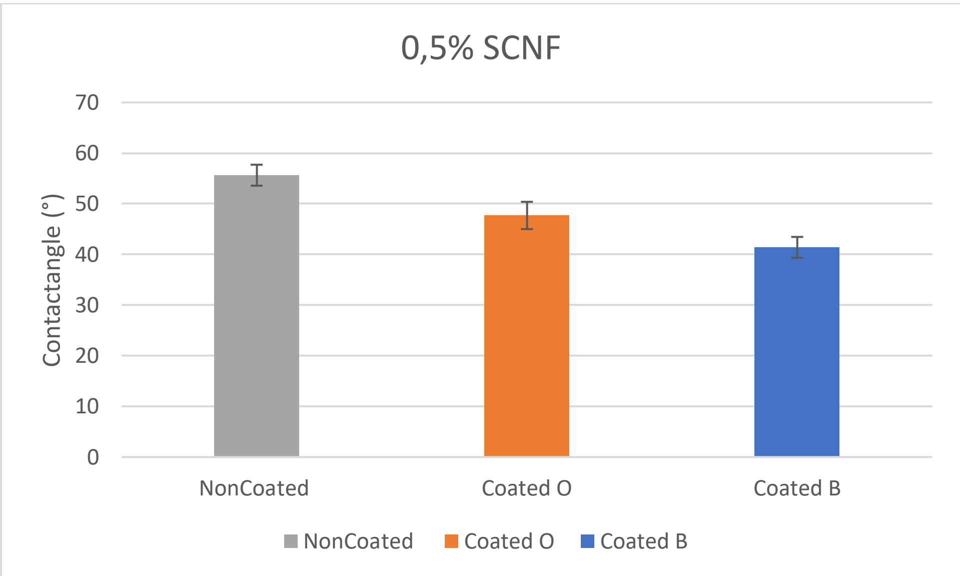

Figure 24: Illustrates the different contact angle values for the noncoated substrate and the two different coating thickness at 0,5% SCNF concentration.

7.6 SEM analysis

The SEM images showed that there are changes in the surface morphology compared to the noncoated substrates. It can also be seen that the lower coating concentration is more uniform than the higher concentration coating. The higher concentration coatings (c) and (d) which can be seen in figure 26 exhibits more variation in thickness, leading to areas being thicker or thinner. The lower concentration coatings (a) and (b) in figure 26 is relatively more uniform.

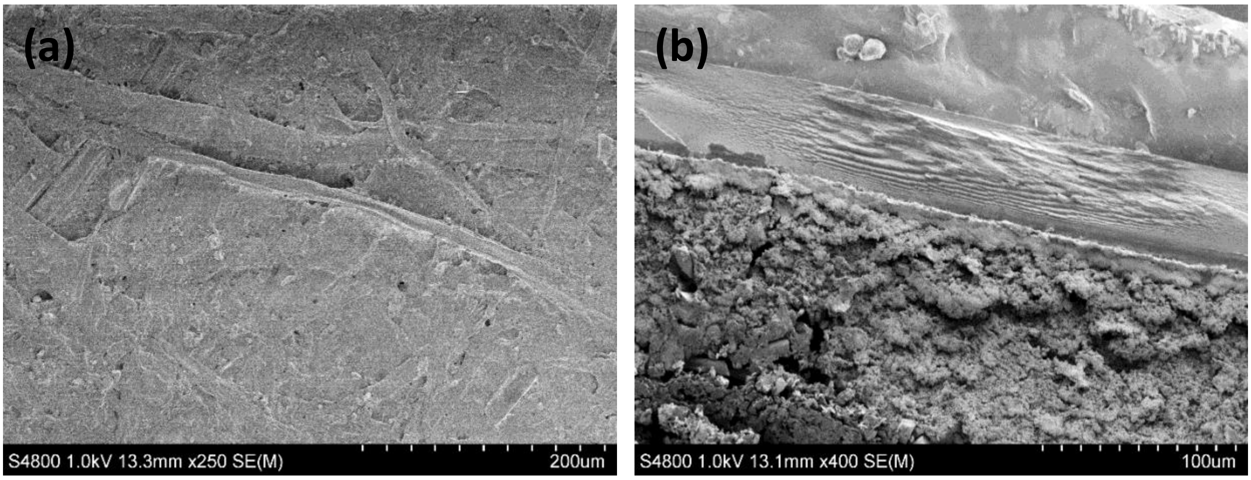

Figure 25: Shows the different scanning electron microscope images for kraft paper (a) and inkjet paper (b).

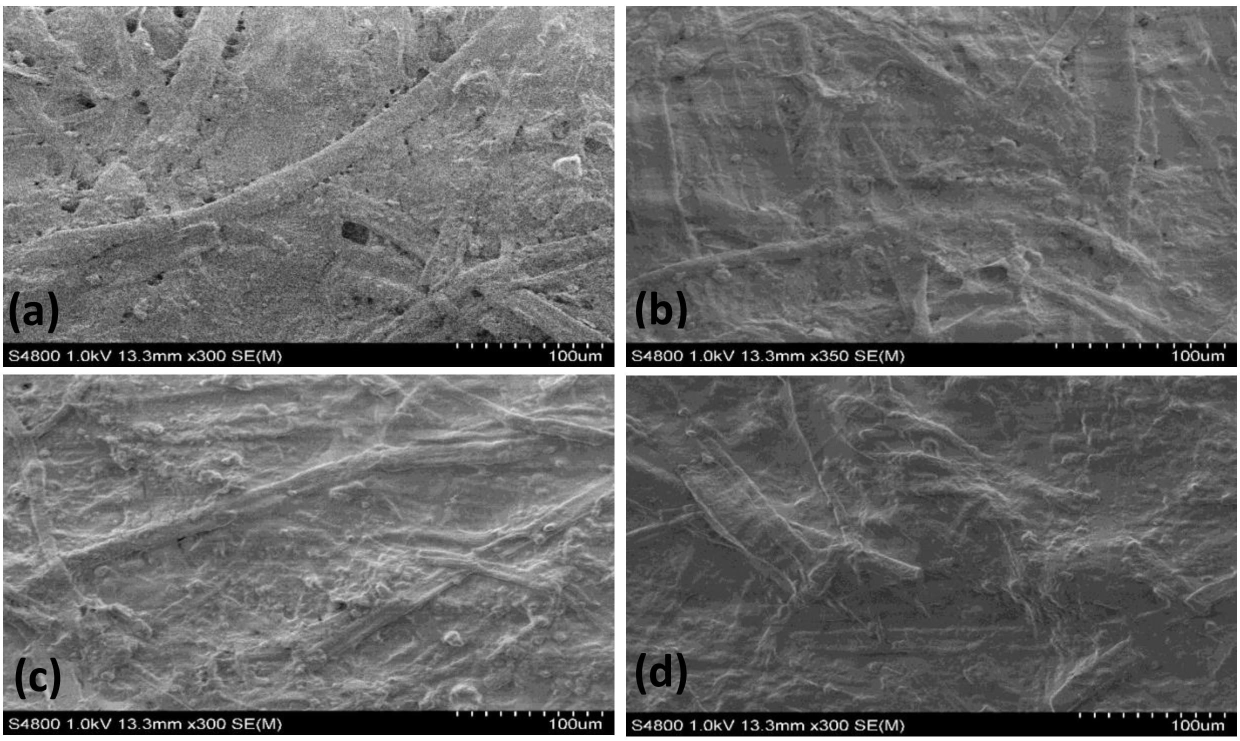

Figure 26: Shows the different scanning electron microscope images for the kraft paper. (a) 0,5% SCNF orange rod, (b) 0,5% SCNF blue rod, (c) 1,5% SNCF orange rod and (d) 1,5% SCNF blue rod.

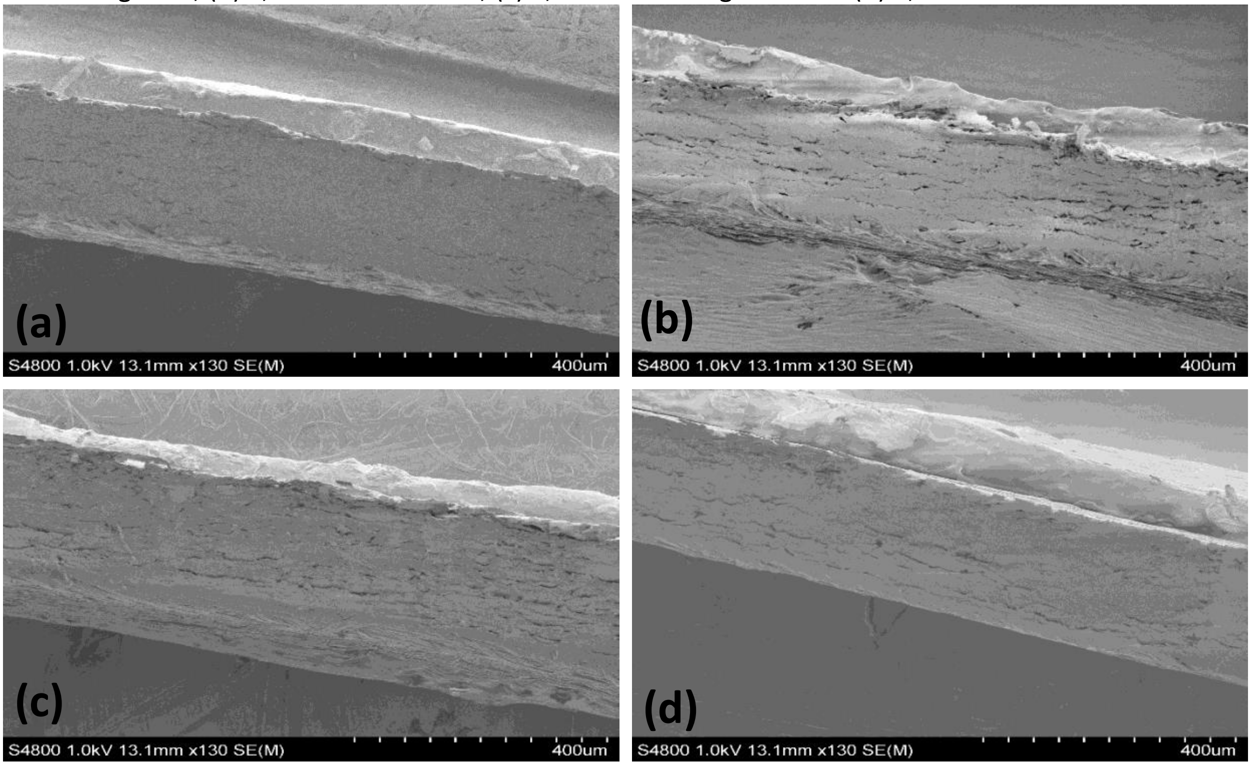

Figure 27: Shows the different scanning electron microscope pictures for the inkjet paper. (a) 0,5% SCNF orange rod, (b) 0,5% SCNF blue rod, (c) 1,5% SNCF orange rod and (d) 1,5% SCNF blue rod

7.7 Ionic conductivity for the coated substrates

The ionic conductivity for the SCNF membrane that was measured as reference for the coated substrates showed a greater ionic conductivity. The ionic conductivity for kraft paper was higher than inkjet paper.

Table 3: Illustrates the ionic conductivity (IC) for the different substrates coated with 1,5% SCNF with the blue rod. The substrates were compared to SCNF membranes without additives.

Sample	Thickness wet (µm)	R_{mem}(Ohm)	IC (mS/cm)	Mean IC (mS/cm)	SD
IP 1,5% Blue A	404	105	0,768		
IP 1,5% Blue B	407	107	0,760		
IP 1,5% Blue C	409	82,7	0,984	**0,837**	**0,104**
K 1,5% Blue A	157	35,2	0,888		
K 1,5% Blue B	151	17,1	1,76		
K 1,5% Blue C	154	24,5	1,25	**1,30**	**0,357**
SCNF reference A	142	12,4	2,27		

SCNF reference B	115	9,40	2,44		
SCNF reference C	136	4,60	5,92	**3,55**	**1,68**

8. Discussion

Coating with SCNF using the rod coater showed promise however an issue was present in the coating process using the rod coater. For some measurements with the lower concentration the rod would not coat the entire surface leaving some small parts uncoated. Even for the inkjet paper regardless of the concentration the whole surface didn't get coated leaving some parts uncoated. The rod coater was calibrated and balanced on each side, but the issue still remained.

The viscosity for the 1,5% SCNF was higher than the lower concentration of 0,5% and this is illustrated in table 1 & 2. This is likely because there are more nanofibrils in the solution which creates more interactions between them and strengthens the overall network of nanofibrils. The viscosity of the SCNF suspensions can also be influenced by the level of sulfonation. The surface area of nanocellulose is great. As a result, there are more intermolecular interactions concentrated there and more frictional forces between the fibers. These elements increase intermolecular contact and flow resistance, which increases the viscosity of nanofibrils (Trache et al 2020). At greater concentrations, the nanofibrils are more closely packed together and the attractive van der Waals forces becomes more dominant.

Concentrations of 1,5% and 0,5% SCNF dispersion was coated onto two different substrates, kraft paper and ink paper using two different rods. The results for ink paper with the two different concentrations can be viewed in figure 9 and 10. For the noncoated ink paper the thickness was around 503μm, coating with the orange rod using 1,5% SNCF concentration the thickness of the paper increased to 532μm and for the blue rod the thickness was measured to be 535μm; a slight increase in thickness. However, for the lower concentration 0,5% SCNF there was the same increase in thickness, but the thickness measured was not as thick, which can be seen in figure 10. Viscosity affects the coating material's leveling and flow characteristics. Coating with a higher viscosity tend to flow more slowly and have less ability to level, resulting in a thicker and less even coating. A thinner and more uniform coating is a result when coating with lower viscosity because they flow more easily and may level off better.

For the noncoated kraft paper the thickness was measured to 374,1μm and for the two different concentrations using two different rods the thickness did not vary that much between each other which can be seen in figure 11 and 12. The coating thickness when using the orange rod showed nearly the same thickness values for both concentrations, the same pattern followed when using the blue rod. The reason for this could be because the viscosity of the SCNF suspension tends to decrease as the shear rate increases on the kraft paper, a characteristic known as shear thinning (Rajesh 2022 et al). In other words, as the coating material is induced by shear forces its viscosity reduces resulting in smoother flow and leveling. Regardless of the SNCF concentration, the shear thinning behavior can reduce the effect of concentration on coating thickness resulting in similar thicknesses. Kraft paper is an absorbent substrate and has the ability to both absorb and spread the coating material. The final coating thickness may change as a result of this absorption. The amount of material absorbed by the substrate may increase with higher SCNF concentrations, reducing the difference in coating thickness between the two concentrations. A source of error for the thickness could also be that the coated substrates would get dented after drying making it difficult to measure the thickness.

In figure 13 and 14 the permeance can be seen for inkjet paper coated with 1,5% or 0,5% SCNF. When measured using the Gurley method, permeability often refers to the material's air permeability. The Gurley method is designed to measure the resistance of a substance's airflow resistance. The Gurley method yields a permeance value that gives characteristics on the material's capacity to resist airflow. It rates how easily or difficultly air may travel through the substance.

The noncoated inkjet papers permeance was measured to be 111,2 Gurley seconds, for the substrate coated with the orange rod the value decreased to 17 Gurley seconds. For the blue rod the PPS machine could not measure the permeance because it was under the lower limit. A lower permeance value indicates more airflow resistance, meaning that the substrate is less permeable to air. A higher permeance value indicates less resistance to air passage which means greater air permeability. The noncoated inkjet paper had a lower resistance to airflow compared to the coated substrates. The permeance of the inkjet paper coated with a blue rod was under the lower limit of the instrument and could therefore not be measured. These results indicate that it was possible to coat the substrates sufficiently homogeneous to provide a significant barrier compared to the bare substrate.

For the 0,5% SCNF coated ink paper the permeance could be measured for the blue coated inkjet paper to 17,3 Gurley seconds. The orange coated substrate showed around the same value for both concentrations. The permeance for the noncoated kraft paper could not be measured due to it being under the low limit value, however the permeance could be measured for the coated substrates yielding around the same values regardless of concentration and coating rod. In general, the permeance values for the different concentrations and different rod usage showed minimal variation in Gurley seconds. There could be a concentration range for the SNCF where permeance doesn’t change much with increasing concentration hence resulting in minimal differences in permeance. Even if there might have been a variation in coating thickness there could have been other coating properties like porosity and density that might have affected permeance. The overall coating structure and porosity may have stayed mostly constant.

The mechanical strength of the kraft paper can be seen in figure 17 and 18, the results show an improvement in tensile strength index, energy absorption and strain at break when the substrate is coated with SCNF, however the tensile stiffness index deteriorated. The reason for the improved properties could be because when the modified nanocellulose is coated on the substrate it can form a strong bond with the paper fibers. This enhanced fiber-fiber improves load transfer mechanisms within the material. This results that the paper can endure greater loads and stresses before failing because of this increased fiber bonding's ability to raise the tensile strength index. The improved ductility and flexibility offered by the modified nanofibrils coating could however lead to a reduction in the paper's overall stiffness and result in a lower tensile stiffness index. The presence of the modified nanocellulose also showed an increase in strain at break which could be because of the coatings ability to enhance interlocking and adhesion, preventing early fiber separation. This also resulted in a higher energy absorption which could be because with the coating it can distribute energy more effectively due to the nanofibrils, it can take more energy before breaking.

In Spagnuolo et al (2022) research coating with CNF resulted enhanced the substrates strength and improved barrier properties. In this thesis however CNF is sulfonated and SCNF is coated. The mechanical strength of the paper did increase with the SCNF coating and the permeance reduced as well for the coated SCNF substrates.

The thicker coating in figure 17 illustrates stronger mechanical properties comparted to the thinner coating. Comparing the results in figure 17 to figure 18 it could be possible that at lower concentrations the thickness of the coating did not improve with a thicker coating using the two different rods, however more testing is required in order to confirm this. There was however an issue with coating at low concentrations that was noticeable on the substrates, the coating material wasn't evenly distributed over the surface leaving a variation across the substrates surface.

In figure 19 and 20 the mechanical strength for the inkjet paper can viewed. The results in figure 19 with the 1,5% SCNF shows nearly similarities in pattern to the kraft paper with 1,5% SCNF. The difference being in tensile stiffness index where the orange rod coated substrates having a higher result in tensile stiffness followed by noncoated and lastly blue coated. For the lower concentration in figure 20 the same issue occurred as the kraft paper which led to the coating material not being evenly distributed.

Studying the results for the contact angle measurement for the kraft paper which is illustrated in figure 21. The noncoated substrate had a significantly much higher contact angle compared to the orange and blue coated kraft papers at 1,5% SCNF concentration. The reason the for the decrease in contact angle for the coated kraft papers might be because of the hydrophilic property of the sulfonated groups present in the nanocellulose. A thicker coating resulted in a slightly lower contact angle compared to the thinner coating. The reason for this could be that a thicker coating layer offers the liquid a broader surface area to interact with, enabling a wider spreading. This may result in a decrease in contact angle and an increase in hydrophilicity. In Guo et al (2018) research the contact angle results on the surface of CNF films was 60,4°. A significantly higher contact angle compared to the substrate coated with 1,5% SCNF, however compared to the lower concentration of 0,5% SCNF the contact angle values are approximately much closer. The reason for this could be as mentioned that the presence of sulfonate groups and a higher concentration result in lower contact angle. In Kock-Yee (2014) study it is revealed that a surface is defined as hydrophobic when its static water contact angle is more than 90° and as hydrophilic when is lower than 90°. The noncoated kraft paper and inkjet paper are considered as hydrophilic however the coated substrates are more hydrophilic due to lower contact angle.

Contact angle of the 0,5% SCNF concentration was rather high for the coated kraft paper which can be seen in figure 22. This could be affected because of the lower concentration; higher concentration of hydrophilic coating materials decreases the contact angle. This is because a higher concentration has a larger density of hydrophilic functional groups, which can improve the interaction between the liquid and the coating. The liquid is therefore more prone to disperse and display a smaller contact angle.

The inkjet paper at 1,5% SCNF in figure 23 showed similar results to that of the 1,5% SCNF kraft paper however the results differed slightly for the 0,5% SCNF concentrations. This may be because the lower concentration of SCNF may not have changed the surface characteristics of both kraft paper and inkjet paper. The concentration might not have been high enough to significantly alter the chemistry of the substrates surfaces resulting in similar contact angles.

SEM images can be seen in figure 25 for the noncoated substrates, (a) being kraft paper and (b) inkjet paper. In figure 26 the SEM images can be viewed for kraft paper and in figure 27 inkjet paper SEM images can be seen. The SEM images showed that there are changes in the surface morphology compared to the noncoated substrates. The lower concentrations seem to be more uniform than the higher concentrations due to higher concentration exhibiting more variation in thickness leading to some areas being thicker or thinner. The coated substrates have more interconnected networks of fibrils.

Ionic conductivity for the 1,5% SCNF blue coated substrates can be seen in table 3 being compared to SCNF membranes as reference. The mean IC for the inkjet paper was calculated to 0,837mS/cm and 1,3mS/cm for the kraft paper. Due to the high thickness, the resistance is quite high for some of the separator samples, the thickness needs to be lower for them to become industrially relevant. The kraft paper had better ionic conductivity compared to the inkjet paper due to inkjet paper being thicker. The SCNF reference membrane had higher ionic conductivity compared to the separators possibly due to the material's advantageous structure and the content of charged groups. In Montibon (2011) research he explains that conducting materials are substances that allow the flow of ions and/or electrons along the structure. In the research it is mentioned that materials can be classified into insulators, semiconductors and conductors based on their conductivities.
The widely used material of separators are polyolefin membranes such as polypropylene (PP) for example. In Mao et al (2021) research PP ionic conductivity was measured to 2,05mS/cm. Kraft paper coated with 1,5% SCNF had an ionic conductivity of 1,30mS/cm which is lower compared to the PP.

It has been demonstrated that SCNF can indeed be used for coating applications and has been evaluated through different experiments. The permeance of the coated samples was tested using the Gurley method to assess the coating's effectiveness. The Gurley technique calculates the amount of time needed for air to move through a specific area of coated material under controlled circumstances. Better barrier qualities are indicated by lower permeance values. Additionally in order to evaluate the coated samples wettability, the contact angle of the samples was determined. A liquid’s ability to spread out or remain on a surface as a sphere is determined by its contact angle. Greater surface wetting and better adhesion characteristics are indicated by a lower contact angle. The results showed that coating with sulfonated cellulose nanofibrils improved wettability and barrier qualities. Lower permeance readings in the coated samples showed greater resistance to the penetration of gases. Additionally, the contact angle measurements revealed decreased contact angles, indicating increased liquid adhesion and surface wetting.

In addition to the previous experiments on coating with SCNF, the mechanical strength of the coated samples was also evaluated. The results provided good insights on the mechanical strength performance of the coated samples. It was found that the presence of SCNF enhanced the mechanical strength compared to the bare substrates.

9. Conclusion

One of the purposes of this thesis was to investigate the possibility of coating with sulfonated nanocellulose on paper substrates, how the different properties of the modified nanocellulose can affect the experiment by changing concentration, thickness and substrate. The result was also investigated through characterization of the coated substrates by surface- and cross-sectional SEM. Investigation on how well the coated substrate can function as separator by ionic conductivity was also an important purpose of this thesis. Coating the paper substrate with modified nanocellulose was possible, however as mentioned earlier at the lower concentration there were some parts of the surface that remained uncoated. Improvements can be made in order to get an even coating surface where the whole surface is coated, through adjusting the rod coater or implementing a different kind of coating technique for instance spray coating. Regardless the results demonstrated that SCNF can indeed be used for coating applications, and this has been supported by the different experiments. For instance, the permeance of the coated samples were tested to assess the coating's effectiveness which revealed to give good barrier properties indicated by lower Gurley permeance values. The SCNF presence in the substrates also showed an improvement in mechanical properties and the presence of SCNF could also be seen with SEM.

The Ionic conductivity is believed to have possibilities for improvement, perhaps through different coating techniques or changing certain parameters. This opens paths for future research on this topic. This could also be tested in zinc ion batteries to view the possibility of using SCNF paper substrates as separators.

10. Future research

Analyzing the results in this thesis some potential on improvements has come to mind. Some improvements in mind could be to try and spray coat the SCNF instead of using a rod coater to study the difference between that and using a rod coater. It could also be interesting to apply this coated substrate as separators in a zinc ion battery to study how they would operate compared to the commercially used materials as separators. It could also be interesting to focus on improving the coating procedure in a rod coater to try and get a very uniform coating on the substrate to study this effect.

Acknowledgments

I would like to express my most sincere appreciation to my two supervisors, Mozhgan Hashemzehi and Sanna Lander for their guidance, patience and encouragement throughout the whole process finalizing this master thesis. Mozhgan was very caring, and I always felt welcomed and appreciated with my questions and concerns. Sanna was very helpful, always trying to make things easier for me and provided me with good insight to this topic.

My final gratitude goes to both my mom and dad always showing me support and love throughout the whole semester working with my thesis. Their encouragement really made things easier for me and this work would not have been possible without them.

References

Al-Amin, M.; Islam, S.; Shibly, S.U.A.; Iffat, S. Comparative Review on the Aqueous Zinc-Ion Batteries (AZIBs) and Flexible Zinc-Ion Batteries (FZIBs). Nanomaterials 2022, 12, 3997. https://doi.org/10.3390/nano12223997

Aulin C, Ahola S, Josefsson P, Nishino T, Hirose Y, Osterberg M, Wågberg L. Nanoscale cellulose films with different crystallinities and mesostructures--their surface properties and interaction with water. Langmuir. 2009 Jul 7;25(13):7675-85. doi: 10.1021/la900323n. PMID: 19348478.

Carpita NC, Gibeaut DM. Structural models of primary cell walls in flowering plants: consistency of molecular structure with the physical properties of the walls during growth. Plant J. 1993 Jan;3(1):1-30. doi: 10.1111/j.1365-313x.1993.tb00007.x. PMID: 8401598.

Chakrabarty, A.; Teramoto, Y. Recent Advances in Nanocellulose Composites with Polymers: A Guide for Choosing Partners and How to Incorporate Them. Polymers 2018, 10, 517. https://doi.org/10.3390/polym10050517

Dieter Klemm, Emily D. Cranston, Dagmar Fischer, Miguel Gama, Stephanie A. Kedzior, Dana Kralisch, Friederike Kramer, Tetsuo Kondo, Tom Lindström, Sandor Nietzsche, Katrin Petzold-Welcke, Falk Rauchfuß, Nanocellulose as a natural source for groundbreaking applications in materials science: Today's state, Materials Today, Volume 21, Issue 7, 2018, https://doi.org/10.1016/j.mattod.2018.02.001

Bayer, T., Cunning, B.V., Šmíd, B. et al Spray deposition of sulfonated cellulose nanofibers as electrolyte membranes in fuel cells. Cellulose 28, 1355–1367 (2021). https://doi.org/10.1007/s10570-020-03593-w

Guo, Jiaqi & Filpponen, Ilari & Johansson, Leena-Sisko & Heiβler, Stefan & Li, Lei & Levkin, Pavel & Rojas, Orlando. (2018). Micro-patterns on nanocellulose films and paper by photo-induced thiol–yne click coupling: a facile method toward wetting with spatial resolution. Cellulose. DOI:10.1007/s10570-017-1593-2

Guozhao Fang, Jiang Zhou, Anqiang Pan, and Shuquan Liang. Recent Advances in Aqueous Zinc-Ion Batteries, ACS Energy Letters 2018 3 (10), 2480-2501 DOI: 10.1021/acsenergylett.8b01426

Habibi, Y. (2014). Key advances in the chemical modification of nanocelluloses. Chemical Society Reviews, 43(5), 1519-1542. https://doi.org/10.1039/C3CS60204D

Hubbe, M. A., Ferrer, A., Tyagi, P., Yin, Y., Salas, C., Pal, L., and Rojas, O. J. (2017). "Nanocellulose in thin films, coatings, and plies for packaging applications: A review," BioRes. 12(1), 2143-2233. DOI: 10.15376/biores.12.1.2143-2233

Jizhang Chen, Minfeng Chen, Hong Ma, Weijun Zhou, Xinwu Xu, Advances and perspectives on separators of aqueous zinc ion batteries, Energy Reviews, 2022 https://doi.org/10.1016/j.enrev.2022.100005.

Jun Ming, Jing Guo, Chuan Xia, Wenxi Wang, Husam N. Alshareef, Zinc-ion batteries: Materials, mechanisms, and applications, Materials Science and Engineering: R: Reports, Volume 135, 2019

Kargarzadeh, H., Mariano, M., Gopakumar, D. A., Ahmad, I., & Thomas, S.. Recent developments in nanocellulose-based biodegradable polymers. Biotechnology Advances, 2018 32(1), 347-365. DOI: 10.1016/j.progpolymsci.2018.07.008

Klemm, D., Kramer, F., Moritz, S., Lindström, T., Ankerfors, M., Gray, D. and Dorris, A. (2011), Nanocelluloses: A New Family of Nature-Based Materials. Angew. Chem. Int. Ed., 50: 5438-5466.

Kock-Yee Law Definitions for Hydrophilicity, Hydrophobicity, and Superhydrophobicity: Getting the Basics right, The Journal of Physical Chemistry Letters 2014 5 (4), 686-688, DOI: 10.1021/jz402762h

Lander, S., Erlandsson, J., Vagin, M., Gueskine, V., Korhonen, L., Berggren, M., Wågberg, L., Crispin, X., Sulfonated Cellulose Membranes: Physicochemical Properties and Ionic Transport versus Degree of Sulfonation. Adv. Sustainable Syst. 2022, 6, 2200275.

Lee, K. Y., Blaker, J. J., Bismarck, A., & Shaffer, M. S.. Functionalised cellulose nanofibrils for improved dispersion in epoxy matrices and impact toughness. Nanoscale, 8(7), 4114-4123. 2016.

Lehrhofer AF, Goto T, Kawada T, Rosenau T, Hettegger H. The in vitro synthesis of cellulose - A mini-review. Carbohydr Polym 2022

Liimatainen, H., Visanko, M., Sirviö, J. A., & Hormi, O. (2012). Combined periodate oxidation and sulfonation enables straightforward preparation of nanocellulose carboxylate and sulfonate. Cellulose, 19(5), 1585-1594.

Mao Yang, Jue Nan, Wei Chen, Anjun Hu, He Sun, Yuanfu Chen, Chunyang Wu, Interfacial engineering of polypropylene separator with outstanding high-temperature stability for highly safe and stable lithium-sulfur batteries, Electrochemistry Communications, Volume 125, 2021, 106971, ISSN 1388-2481, https://doi.org/10.1016/j.elecom.2021.106971.

Montibon, E. (2011). Modification of Paper into Conductive Substrate for Electronic Functions: Deposition, Characterization and Demonstration. (Doctoral dissertation). Karlstad: Karlstad University

Moon RJ, Martini A, Nairn J, Simonsen J, Youngblood J. Cellulose nanomaterials review: structure, properties and nanocomposites. Chem Soc Rev. 2011 Jul;40(7):3941-94. doi: 10.1039/c0cs00108b. Epub 2011 May 12. PMID: 21566801.

Muhmed, S.A., Nor, N.A.M., Jaafar, J. et al. Emerging chitosan and cellulose green materials for ion exchange membrane fuel cell: a review. Energ. Ecol. Environ. 5, 85–107 (2020).

Nanoscale cellulose films with different crystallinities and mesostructures—Their surface properties and interaction with water 2009

Noack, J.; Wietschel, L.; Roznyatovskaya, N.; Pinkwart, K.; Tübke, J. Techno-Economic Modeling and Analysis of Redox Flow Battery Systems. Energies 2016, 9, 627.

Polko JK, Kieber JJ. The Regulation of Cellulose Biosynthesis in Plants. Plant Cell. 2019 Feb;31(2):282-296. doi: 10.1105/tpc.18.00760. Epub 2019 Jan 15. PMID: 30647077; PMCID: PMC6447023.

Prifti, H.; Parasuraman, A.; Winardi, S.; Lim, T.M.; Skyllas-Kazacos, M. Membranes for Redox Flow Battery Applications. Membranes 2012, 2, 275-306.

R.S.L. Yee, R.A. Rozendal, K. Zhang, B.P. Ladewig, Cost effective cation exchange membranes: Chemical Engineering Research and Design, Volume 90, Issue 7,2012,

Rajesh Koppolu, Gabriel Banvillet, Himal Ghimire, Julien Bras, and Martti Toivakka Enzymatically Pretreated High-Solid-Content Nanocellulose for a High-Throughput Coating Process, ACS Applied Nano Materials 2022 5 (8), 11302-11313 doi: 10.1021/acsanm.2c02423

Reeba Mary Cherian, Abhimanyu Tharayil, Rini Thresia Varghese, Tijo Antony, Hanieh Reshmy R, Philip E, Thomas D, Madhavan A, Sindhu R, Binod P, Varjani S, Awasthi MK, Pandey A. Bacterial nanocellulose: engineering, production, and applications. Bioengineered. 2021

Shuo Huang, Jiacai Zhu, Prof. Jinlei Tian, Prof. Zhiqiang Niu. Recent Progress in the Electrolytes of a Aqueous Zinc-Ion Batteries 2019, 25, 14480, https://doi.org/10.1002/chem.201902660

Spagnuolo L, D'Orsi R, Operamolla A, Nanocellulose for Paper and Textile Coating: The Importance of Surface Chemistry ChemPlusChem 2022, 87 DOI: https://doi.org/10.1002/cplu.202200204

Somerville, Chris & Bauer, Stefan & Brininstool, Ginger & Facette, Michelle & Hamann, Thorsten & Milne, Jennifer & Osborne, Erin & Paredez, Alexander & Persson, Staffan & Raab, Ted & Vorwerk, Sonja & Youngs, Heather. (2005). Toward a Systems Approach to Understanding Plant Cell Walls. Science (New York, N.Y.). 306. 2206-11. 10.1126/science.1102765.

Syverud, K., Stenius, P., & Gällstedt, M. Cellulose nanofibrils: challenges and possibilities as a coating material. Paperi ja Puu-Paper and Timber, (2013) 95(1), 30-35.

T. Bayer, B. V. Cunning, R. Selyanchyn, M. Nishihara, S. Fujikawa, K. Sasaki, S. M. Lyth, Chem. Mater. High Temperature Proton Conduction in Nanocellulose Membranes: Paper Fuel Cell, 2016, 28, 4805.

Tiina Nypelö, Barbara Berke, Stefan Spirk, Juho Antti Sirviö. Periodate oxidation of wood polysaccharides—Modulation of hierarchies, Carbohydrate Polymers, Volume 252, 2021

Trache Djalal, Tarchoun Ahmed Fouzi, Derradji Mehdi, Hamidon Tuan Sherwyn, Masruchin Nanang, Brosse Nicolas, Hussin M. Hazwan, Nanocellulose: From Fundamentals to Advanced Applications, DOI=10.3389/fchem.2020.00392m, Frontiers in Chemistry Volume 1, Issue 1, 2022, 100005, ISSN 2772-9702f

Xiaolong leng, Mungai Yang, Changping Li, Waqas UI Arifeen, Tae Jo Ko,. High-performance separator for lithium-ion battery based on dual-hybridizing of materials and processes. Chemical Engineering Journal Volume 433, Part 3, 2022, 133773, ISSN 1385-8947 https://doi.org/10.1016/j.cej.2021.133773.

Zhenglin Li, Lei Ye, Guoqiang Zhou, Wangwang Xu, Kangning Zhao, Xiaoman Zhang, Shu Hong, Tongtong Ma, Mei-Chun Li, Chaozheng Liu, Changtong Mei, A water-gating and zinc-sieving lignocellulose nanofiber separator for dendrite-free rechargeable aqueous zinc ion battery, Chemical Engineering Journal 2023, 457, 141160, https://doi.org/10.1016/j.cej.2022.141160